
Bridging the Gap Between Practice and PAC-Bayes Theory in Few-Shot Meta-Learning

Nan Ding
Google Research
Venice, CA 90291
dingnan@google.com

Xi Chen*
Harvard University
Cambridge, MA 02138
xichenpkuphy@gmail.com

Tomer Levinboim
Google Research
Venice, CA 90291
tomerl@google.com

Sebastian Goodman
Google Research
Venice, CA 90291
seabass@google.com

Radu Soricut
Google Research
Venice, CA 90291
rsoricut@google.com

Abstract

Despite recent advances in its theoretical understanding, there still remains a significant gap in the ability of existing PAC-Bayesian theories on meta-learning to explain performance improvements in the few-shot learning setting, where the number of training examples in the target tasks is severely limited. This gap originates from an assumption in the existing theories which supposes that the number of training examples in the observed tasks and the number of training examples in the target tasks follow the same distribution, an assumption that rarely holds in practice. By relaxing this assumption, we develop two PAC-Bayesian bounds tailored for the few-shot learning setting and show that two existing meta-learning algorithms (MAML and Reptile) can be derived from our bounds, thereby bridging the gap between practice and PAC-Bayesian theories. Furthermore, we derive a new computationally-efficient PACMAML algorithm, and show it outperforms existing meta-learning algorithms on several few-shot benchmark datasets.

1 Introduction

Recent advances in machine learning and neural networks have resulted in effective but parameter-bloated, data-hungry models. When the training data for a target task of interest is insufficient, such overparameterized models may easily overfit to the training data and exhibit poor generalization abilities. To address this problem, several research efforts have focused on designing a learning strategy that can leverage the training data of other tasks for the sake of improving the performance of some specific target task(s). Specifically, in the meta-learning (also called learning-to-learn or lifelong-learning) setting [Baxter, 1998, Ravi and Larochelle, 2017], a meta-learner first extracts knowledge from a set of observed (meta-training) tasks and subsequently, this knowledge enables a base-learner to better adapt to the new, possibly data-limited target (meta-testing) task. The meta-learning framework has been successfully applied and made significant practical impact on computer vision [Russakovsky et al., 2015], language understanding [Devlin et al., 2019], reinforcement learning [Finn et al., 2017] and many other research fields.

In parallel to its impressive empirical success, a series of theoretical works [Tripuraneni et al., 2020, Pentina and Lampert, 2014, Amit and Meir, 2018, Rothfuss et al., 2020] study how meta-learning utilizes the knowledge obtained from the observed task data and how it generalizes to the unseen

*Part of work was done during the internship at Google.

target task. Among the generalization bounds, PAC-Bayes bounds [McAllester, 1999, Germain et al., 2009] are considered especially tight and have already been proposed for meta-learning [Pentina and Lampert, 2014, Amit and Meir, 2018, Rothfuss et al., 2020]. However, there still remains a gap between these existing PAC-Bayesian bounds and their practical application (especially in the few-shot setting), which originates from the assumption that the observed task environment \tilde{T} and the target task environment T are the same. In the PAC-Bayesian meta-learning setting, a task environment T is a distribution from which (D, m) is drawn from, where D is the data distribution and m is the number of training examples for the task. Although there is research work studying the case of general environment change (e.g. [Pentina and Lampert, 2015]) or data domain change (e.g. Germain et al. [2016b]), to the best of our knowledge, there is little work focusing on the case where only the number of training examples \tilde{m} in the observed tasks and m in the target task do not follow the same distribution. In practice, such mismatch commonly happens, because there is usually significantly more data in observed tasks than the target tasks, especially in the few-shot case. Without explicitly addressing this mismatch, the scope of the current theory is severely limited, and it prohibits a useful analysis on practical meta-learning algorithms such as MAML Finn et al. [2017]. For example, when the number of training examples m in the target task is small, the existing bounds yield a large generalization gap which grows with $O(1/m)$. In this paper, we bring the theory closer to practice by studying the setting where there are significantly more training examples in the observed task than in the target task (i.e., $\tilde{m} \gg m$). In Section 3.1, we study two practical meta-training strategies and provide their PAC-Bayesian bounds in Theorem 3 and Theorem 4. Both results are able to bring down the scaling coefficient of the bound from $O(1/m)$ to $O(1/\tilde{m})$. However, Theorem 3 introduces a penalty term in the bound that captures the discrepancy between the observed and target task environment. Motivated by MAML Finn et al. [2017], we show with Theorem 4 that we can eliminate the penalty term by utilizing a subsampling strategy, yielding a much tighter bound.

This theoretical work also bridges the gap from practice to theory, as we further show that the maximum-a-posteriori (MAP) estimates of our bounds (in which the base-learner and the hyper-posterior are both approximated by Dirac-measures) yield various popular meta-learning algorithms, including multi-task pretraining [Russakovsky et al., 2015], Reptile [Nichol et al., 2018] and MAML [Finn et al., 2017]. In that sense, our PAC-Bayesian theories provide a different perspective for understanding and justifying these commonly used algorithms (Section 3.2).

Lastly, in Section 4, we propose PACMAML, a novel PAC-Bayesian meta-learning algorithm based on Theorem 4. As opposed to MAML, our algorithm does not have higher-order derivatives in the gradient, and therefore represents a significant improvement in computational efficiency. In Section 5, we conduct numerical experiments that empirically support the correctness of our theorems, and report the effectiveness of the new PACMAML algorithm, which obtains superior results on several few-shot benchmark datasets.

2 Preliminaries

We begin by reviewing the background and settings of the existing PAC-Bayesian bounds for meta-learning. Our notation mainly follows that of [Rothfuss et al., 2020], which is itself adapted from [Pentina and Lampert, 2014, Amit and Meir, 2018, Baxter, 1998].

PAC-Bayesian for Supervised Learning In supervised learning, a learning task is characterized by a data distribution D over a data domain Z where every example $z = (x, y)$. A hypothesis h from the hypothesis space H allows us to make predictions based on inputs x . The quality of the predictions is measured by a loss function $l(h, z)$, where the goal is to minimize the expected loss $L(h, D) = \mathbb{E}_{z \sim D} l(h, z)$. Typically, D is unknown and instead we are given a set of m observations $S \sim D^m = \{z_i \sim D\}_{i=1}^m$, in which case the empirical error on S is simply $\hat{L}(h, S) = \frac{1}{m} \sum_{i=1}^m l(h, z_i)$.

In the PAC-Bayesian setting, we assume that the learner has prior knowledge of the hypothesis space H in the form of a prior distribution $P(h)$. When the learner observes a training dataset S , it updates the prior into a posterior distribution Q . We formalize such a *base learner* $Q(S, P)$ that takes a dataset and a prior as input and outputs a posterior.

The expected error of the posterior Q is called the Gibbs error $L(Q, D) = \mathbb{E}_{h \sim Q} L(h, D)$, and its empirical counterpart is $\hat{L}(Q, S) = \mathbb{E}_{h \sim Q} \hat{L}(h, S)$. The PAC-Bayesian framework provides the following bound over $L(Q, D)$ based on its empirical estimate $\hat{L}(Q, S)$.

Theorem 1 ([Alquier et al., 2016, Germain et al., 2009]) *Given a data distribution D , a hypothesis space H , a prior P , a confidence level $\delta \in (0, 1]$, and $\beta > 0$, with probability at least $1 - \delta$ over samples $S \sim D^m$, we have for all posterior Q ,*

$$L(Q, D) \leq \hat{L}(Q, S) + \frac{1}{\beta} \left(D_{KL}(Q \| P) + \log \frac{1}{\delta} \right) + \frac{m}{\beta} \Psi\left(\frac{\beta}{m}\right) \quad (1)$$

where $\Psi(\beta) = \log \mathbb{E}_{h \sim P} \mathbb{E}_{z \sim D} \exp(\beta(l(h, z) - L(h, D)))$.

PAC-Bayesian for Meta-Learning In the meta-learning setting, the meta-learner observes different tasks $\tau_i = (D_i, m_i)$ during the meta-training stage, where all tasks share the same data domain Z , hypothesis space H and loss function $l(h, z)$. For each observed task τ_i , the meta-learner observes a training set S_i of size m_i which is assumed to be sampled i.i.d. from its respective data distribution D_i (that is, $S_i \in D_i^{m_i}$). We further assume that each task $\tau_i = (D_i, m_i)$ is drawn i.i.d. from an environment T , which itself is a probability distribution over the data distributions and the sample sizes. The goal of meta-learning is to extract knowledge from the observed tasks τ_i , which can then be used as prior knowledge for learning on new (yet unobserved) target tasks $\tau = (D, m) \sim T$. This prior knowledge is represented as a prior distribution $P(h)$ over learning hypotheses h , and it is subsequently used by the base learner $Q(S, P)$ for inference over the target tasks.

In the meta-learning PAC-Bayes framework, the meta-learner presumes a hyper-prior $\mathcal{P}(P)$ as a distribution over priors P . Upon observing datasets S_1, \dots, S_n from multiple tasks, the meta-learner updates the hyper-prior to a hyper-posterior $\mathcal{Q}(P)$. The performance of this hyper-posterior, also called the transfer-error, is measured as the expected Gibbs error when sampling priors P from \mathcal{Q} and applying the base learner:

$$R(\mathcal{Q}, T) := \mathbb{E}_{P \sim \mathcal{Q}} \mathbb{E}_{(D, m) \sim T} \mathbb{E}_{S \sim D^m} [L(Q(S, P), D)]. \quad (2)$$

While $R(\mathcal{Q}, T)$ is unknown in practice, it can be estimated using the empirical error,

$$\hat{R}(\mathcal{Q}, S_{i=1}^n) := \mathbb{E}_{P \sim \mathcal{Q}} \left[\frac{1}{n} \sum_{i=1}^n \hat{L}(Q(S_i, P), S_i) \right]. \quad (3)$$

In [Pentina and Lampert, 2014, Rothfuss et al., 2020], the following PAC-Bayesian meta-learning bound is provided:

Theorem 2 ([Pentina and Lampert, 2014, Rothfuss et al., 2020]) *Given a task environment T and a set of n observed tasks $(D_i, m_i) \sim T$, let \mathcal{P} be a fixed hyper-prior and $\lambda > 0$, $\beta > 0$, with probability at least $1 - \delta$ over samples $S_1 \in D_1^{m_1}, \dots, S_n \in D_n^{m_n}$, we have, for all base learner Q and all hyper-posterior \mathcal{Q} ,*

$$\begin{aligned} R(\mathcal{Q}, T) &\leq \hat{R}(\mathcal{Q}, S_{i=1}^n) + \left(\frac{1}{\lambda} + \frac{1}{n\beta} \right) D_{KL}(\mathcal{Q} \| \mathcal{P}) \\ &\quad + \frac{1}{n\beta} \sum_{i=1}^n \mathbb{E}_{P \sim \mathcal{Q}} [D_{KL}(Q(S_i, P) \| P)] + C(\delta, \lambda, \beta, n, m_i). \end{aligned} \quad (4)$$

Here $C(\delta, \lambda, \beta, n, m_i)$ contains Ψ and $\frac{1}{\delta}$ terms as in Eq.(1) (see Appendix A.1), and can be bounded by a function that is independent of \mathcal{Q} for both bounded and unbounded loss functions under moment constraints (see details in [Rothfuss et al., 2020]). From a Bayesian perspective, meta-learning attempts to learn a good hyper-posterior \mathcal{Q} such that for all tasks in the task environment T , the divergence terms $D_{KL}(Q(S_i, P) \| P)$ would be substantially smaller in expectation when $P \sim \mathcal{Q}$ compared to when $P \sim \mathcal{P}$, such as in the ordinary supervised learning setting of Eq.(1).

The hyperparameters λ and β can be adjusted to balance between the first three terms of the bound and the C function. Defining the harmonic mean of m_i as $\tilde{m} = (\sum_{i=1}^n 1/nm_i)^{-1}$, a common choice is $\lambda \propto n$ and $\beta \propto \tilde{m}^\dagger$. In this case, the generalization gap $R(\mathcal{Q}, T) - \hat{R}(\mathcal{Q}, S_{i=1}^n)$ becomes at least $O(\frac{1}{\tilde{m}})$ (from the 3rd-term on the RHS of Eq.4). In the next section, we examine an assumption in this bound which makes it impractical for the few-shot setting.

[†] Another common choice is $\lambda \propto \sqrt{n}$ and $\beta \propto \sqrt{\tilde{m}}$, so that the bound is asymptotically consistent, and scales with $O(\frac{1}{\sqrt{\tilde{m}}})$. However, in practice the bound with $\beta \propto \tilde{m}$ is usually tighter [Germain et al., 2016a].

3 Bridging the Gap between Practice & Theory of Few-Shot Meta-Learning

The previous PAC-Bayesian meta-learning bound (Theorem 2) assumes that the number of training examples m_i for the observed tasks τ_i and the number of training examples m for the target task τ are drawn from the same distribution (i.e. $\mathbb{E}_T[m_i] = \mathbb{E}_T[m]$). However, practical applications of meta-learning such as [Russakovsky et al., 2015, Devlin et al., 2019] operate in a setting where there are far more training examples in the observed tasks than in the target task. Moreover, focusing on the few-shot setting (where m is particularly small) exposes a gap between theory and practice – Theorem 2 is unable to use the large number of observed samples and can only produce a loose bound of $O(\frac{1}{m})$ which is ineffective at explaining the impressive generalization performance of meta-learning as reported in practice.

In this section we attempt to close this gap by deriving an effective PAC-Bayesian bound (Theorem 4) tailored for the few-shot setting. Interestingly, the bounds derived in this section also provide PAC-Bayesian justifications for two practical algorithms, Reptile and MAML.

3.1 Practical PAC-Bayesian Bounds for Few-Shot Meta-Learning

A first attempt at leveraging the larger number of examples m_i in the observed tasks is to directly follow the learning strategy of Theorem 2, by bounding $R(\mathcal{Q}, T)$ using the empirical risk $\hat{R}(\mathcal{Q}, S_{i=1}^n)$, with $S_i \in D_i^{m_i}$ and $(D_i, m_i) \sim \tilde{T}$, despite the change of task environment from T to \tilde{T} . This slight generalization leads to the following bound (with proof in Appendix A.2):

Theorem 3 *For a target task environment T and an observed task environment \tilde{T} where $\mathbb{E}_{\tilde{T}}[D] = \mathbb{E}_T[D]$ and $\mathbb{E}_{\tilde{T}}[m] \geq \mathbb{E}_T[m]$, let \mathcal{P} be a fixed hyper-prior and $\lambda > 0$, $\beta > 0$, then with probability at least $1 - \delta$ over samples $S_1 \in D_1^{m_1}, \dots, S_n \in D_n^{m_n}$ where $(D_i, m_i) \sim \tilde{T}$, we have, for all base learners Q and hyper-posterior \mathcal{Q} ,*

$$R(\mathcal{Q}, T) \leq \hat{R}(\mathcal{Q}, S_{i=1}^n) + \left(\frac{1}{\lambda} + \frac{1}{n\beta}\right) D_{KL}(\mathcal{Q} \| \mathcal{P}) + \frac{1}{n\beta} \sum_{i=1}^n \mathbb{E}_{P \sim \mathcal{Q}} [D_{KL}(Q(S_i, P) \| P)] + C(\delta, \lambda, \beta, n, m_i) + \Delta_\lambda(\mathcal{P}, T, \tilde{T}), \quad (5)$$

where $\Delta_\lambda(\mathcal{P}, T, \tilde{T}) = \frac{1}{\lambda} \log \mathbb{E}_{P \in \mathcal{P}} e^{\lambda(R(P, T) - R(P, \tilde{T}))}$.

When $\mathbb{E}_{\tilde{T}}[\tilde{m}] = \mathbb{E}_{\tilde{T}}[m_i] \gg \mathbb{E}_T[m]$, this decoupling of the task environments seems beneficial at first, because $O(\frac{1}{\tilde{m}})$ is smaller compared to Eq.(4) when $\beta \propto \tilde{m}$. Unfortunately however, Eq.(5) introduces an additional penalty term Δ_λ , which increases as $\mathbb{E}_{\tilde{T}}[\tilde{m}]$ gets larger.

To understand the influence of Δ_λ , we plot the (blue) bound of Eq.(5) in Fig.1 by using the synthetic Sinusoid regression task (see details in Section 5.1 and in Appendix D.4) where we fixed $m = 5$ and varied m_i from 5 to 100. When $m_i = m = 5$, Eq.(5) reduces to Eq.(4) and $\Delta_\lambda = 0$. Contrary to intuition, increasing m_i does not reduce the bound, but instead makes it worse due to the rapid increase of Δ_λ .

Can we utilize more training examples without introducing a penalty term such as Δ_λ ? In the definition of $\hat{R}(\mathcal{Q}, S_{i=1}^n)$ (Eq.(3)), we note that the training dataset S_i of the observed task τ_i is used twice: first in training the base-learner $Q(S_i, P)$, and then, in evaluating the empirical risk $\hat{L}(Q, S_i)$. In analyzing the proof of the theorem (see Appendix A.2), it can be seen that the penalty term arises exactly because $Q(S_i, P)$ is trained over more samples compared to $Q(S, P)$ of the target task.

This motivates us to develop a MAML-inspired learning strategy, in which we maintain the same target-task training environment T for the base-learners of the observed tasks: we first sample a subset $S'_i \in D_i^{m'_i}$ from S_i where $\mathbb{E}[m'_i] = \mathbb{E}_T[m] < \mathbb{E}_{\tilde{T}}[m_i]$ and then use only the subset S'_i to train the base-learner $Q(S'_i, P)$. At the same time, all examples of $S_i \in D_i^{m_i}$ are used for evaluating the empirical risk $\hat{L}(Q, S_i)$, so that the larger m_i in the empirical risk $\hat{L}(Q, S_i)$ help tightening the generalization gap. This new strategy leads to the following bound (proof in Appendix A.3):

Theorem 4 *For a target task environment T and an observed task environment \tilde{T} where $\mathbb{E}_{\tilde{T}}[D] = \mathbb{E}_T[D]$ and $\mathbb{E}_{\tilde{T}}[m] \geq \mathbb{E}_T[m]$, let \mathcal{P} be a fixed hyper-prior and $\lambda > 0$, $\beta > 0$, then with probability*

at least $1 - \delta$ over samples $S_1 \in D_1^{m_1}, \dots, S_n \in D_n^{m_n}$ where $(D_i, m_i) \sim \tilde{T}$, and subsamples $S'_1 \in D_1^{m'_1} \subset S_1, \dots, S'_n \in D_n^{m'_n} \subset S_n$, where $\mathbb{E}[m'_i] = \mathbb{E}_T[m]$, we have, for all base learner Q and all hyper-posterior \mathcal{Q} ,

$$R(\mathcal{Q}, T) \leq \mathbb{E}_{P \sim \mathcal{Q}} \left[\frac{1}{n} \sum_{i=1}^n \hat{L}(Q(S'_i, P), S_i) \right] + \left(\frac{1}{\lambda} + \frac{1}{n\beta} \right) D_{KL}(\mathcal{Q} \| \mathcal{P}) + \frac{1}{n\beta} \sum_{i=1}^n \mathbb{E}_{P \sim \mathcal{Q}} [D_{KL}(Q(S'_i, P) \| P)] + C(\delta, \lambda, \beta, n, m_i). \quad (6)$$

This bound is still $O(\frac{1}{\tilde{m}})$ when choosing $\beta \propto \tilde{m}$, but unlike Eq.(5), it does not have an additional penalty term in Eq.(6), which is due to the shared training environment T of the base-learners in both observed and target tasks. Importantly, the resulting bound is effective in the few-shot setting as an increase in the number of observed examples m_i monotonically tightens the generalization gap. This is visually demonstrated in Fig.1 in which the (orange) bound of Eq.(6) in Theorem 4 is monotonically decreasing as m_i increases, while the bound in Theorem 2 is limited only to $m_i = 5$ and the bound of Theorem 3 grows.

3.2 Justifying Reptile and MAML using PAC-Bayesian Bounds

It is worth noting that Theorems 3 and 4 not only address more practical scenarios in which observed (meta-training) examples are more abundant than the target examples, but they also serve as a justification for popular and practical meta-learning algorithms: Reptile [Nichol et al., 2018] and MAML [Finn et al., 2017].

To show this, let us consider the maximum-a-posteriori (MAP) approximations on the hyper-posterior $\mathcal{Q}(P)$ and base-learner $Q_i(h), \forall i = 1, \dots, n$, with Dirac measures. In addition, we use the isotropic Gaussian priors with variance hyperparameter σ_0^2 and σ^2 for the hyper-prior $\mathcal{P}(P)$ and the prior $P(h)$. The hypothesis h is parameterized by \mathbf{v} . Then we have

$$\mathcal{P}(P) = \mathcal{N}(\mathbf{p} | 0, \sigma_0^2), \quad \mathcal{Q}(P) = \delta(\mathbf{p} = \mathbf{p}_0), \quad P(h_{\mathbf{v}}) = \mathcal{N}(\mathbf{v} | \mathbf{p}, \sigma^2), \quad \mathcal{Q}(h_{\mathbf{v}}) = \delta(\mathbf{v} = \mathbf{q}_i)$$

and the goal of MAP approximation is to find the optimal meta-parameters \mathbf{p}_0 . With the above assumptions, the PAC-Bayesian bound (denoted PacB) of Eq.(5) and Eq.(6) with respect to \mathbf{p}_0 becomes (up to a constant, see Appendix B),

$$PacB(\mathbf{p}_0) = \frac{1}{n} \sum_{i=1}^n \hat{L}(\mathbf{q}_i, S_i) + \frac{\tilde{\xi} \|\mathbf{p}_0\|^2}{2\sigma_0^2} + \frac{1}{n\beta} \sum_{i=1}^n \frac{\|\mathbf{p}_0 - \mathbf{q}_i\|^2}{2\sigma^2}, \quad (7)$$

where $\tilde{\xi} = \frac{1}{\lambda} + \frac{1}{n\beta}$. Here, \mathbf{q}_i can be any function of \mathbf{p}_0 and S_i for Eq.(5) (or \mathbf{p}_0 and S'_i for Eq.(6)), such that the only free variable in Eq.(7) is \mathbf{p}_0 . Indeed, by setting \mathbf{q}_i according to the choices below, we can derive the gradients of several meta-learning algorithms.

When $\mathbf{q}_i = \mathbf{p}_0$, the gradient of Eq.(7) reduces to that of multi-task pretraining [Russakovsky et al., 2015, Devlin et al., 2019],

$$\lim_{\mathbf{q}_i \rightarrow \mathbf{p}_0} \frac{d(PacB)}{d\mathbf{p}_0} = \frac{\tilde{\xi} \mathbf{p}_0}{\sigma_0^2} + \frac{1}{n} \sum_{i=1}^n \frac{d}{d\mathbf{p}_0} \hat{L}(\mathbf{p}_0, S_i).$$

On the other hand, if we use the optimal Dirac-base-learner \mathbf{q}_i^* of \mathbf{p}_0 and S_i , such that

$$\mathbf{q}_i^* = \operatorname{argmin}_{\mathbf{q}_i} \left[\hat{L}(\mathbf{q}_i, S_i) + \frac{\|\mathbf{p}_0 - \mathbf{q}_i\|^2}{2\beta\sigma^2} \right], \quad (8)$$

then the gradient of Eq.(7) becomes substantially simpler (see details in the Appendix B),

$$\frac{d(PacB)}{d\mathbf{p}_0} = \frac{\tilde{\xi} \mathbf{p}_0}{\sigma_0^2} + \frac{1}{n} \sum_{i=1}^n \frac{\mathbf{p}_0 - \mathbf{q}_i^*}{\beta\sigma^2}, \quad (9)$$

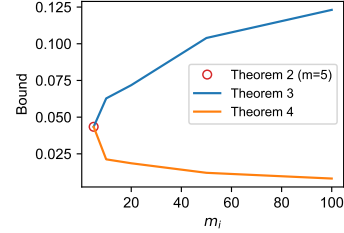


Figure 1: The PAC-Bayesian bounds of Theorems 2, 3, & 4 as evaluated over the Sinusoid dataset. Some constant terms are neglected (see Appendix D.4 for more details).

and in fact, Eq.(9) is equivalent to the meta-update rule of the Reptile algorithm [Nichol et al., 2018], whose inner-loop is an approximate algorithm for solving the optimal Dirac-base-learner \mathbf{q}_i^* .

Lastly, when \mathbf{q}_i is a few gradient descent steps of $\hat{L}(\mathbf{q}_i, S'_i)$ with initial $\mathbf{q}_i = \mathbf{p}_0$, the gradient of Eq.(7) reduces to that of the MAML algorithm[‡] [Finn et al., 2017] as $\sigma^2 \rightarrow \infty$,

$$\lim_{\sigma^2 \rightarrow \infty} \frac{d(\text{PacB})}{d\mathbf{p}_0} = \frac{\tilde{\xi} \mathbf{p}_0}{\sigma_0^2} + \frac{1}{n} \sum_{i=1}^n \frac{d}{d\mathbf{p}_0} \hat{L}(\mathbf{q}_i, S_i).$$

One observation here is that, since \mathbf{q}_i is function of the gradient of \mathbf{p}_0 , $d\mathbf{q}_i/d\mathbf{p}_0$ involves high-order gradient w.r.t. \mathbf{p}_0 , which would result in a computationally intensive algorithm. In the next section we present a computationally efficient algorithm which relies only on first-order derivatives.

4 PAC-Bayesian Meta-Learning Algorithms in the Few-Shot Setting

In this section we present two PAC-Bayesian based Meta-Learning algorithms with non-Dirac base-learners. We first derive their objective functions from the RHS of Eq.(5) and Eq.(6), and then derive low-variance gradient estimators for their optimization.

First, since Eq.(4) and Eq.(5) only differ by Δ_λ , we follow [Rothfuss et al., 2020] and plug in their proposed Gibbs posterior based base-learner $Q^*(S_i, P)(h) = P(h) \exp(-\beta \hat{L}(h, S_i)) / Z_\beta(S_i, P)$ into Eq.(5), which minimizes Eq.(5) w.r.t. Q . This yields that, with at least $1 - \delta$ probability,

$$R(Q, T) \leq \frac{1}{n} \sum_{i=1}^n \mathbb{E}_{P \sim \mathcal{Q}} \underbrace{\left[-\frac{1}{\beta} \log Z_\beta(S_i, P) \right]}_{W_1} + \tilde{\xi} D_{KL}(Q \| \mathcal{P}) + \Delta_\lambda + C \quad (10)$$

where $\tilde{\xi} = \frac{1}{\lambda} + \frac{1}{n\beta}$ and C is the same constant from the previous bounds. Since Δ_λ is independent of \mathcal{Q} and can be neglected during inference or optimization of \mathcal{Q} , it reduces to the same PACOH objective as in [Rothfuss et al., 2020].

On the other hand, the same Gibbs posterior cannot be used as the base learner of Eq.(6), because the Gibbs posterior would depend on S_i , while the base learner in Eq.(6) should only be dependent on $S'_i \subset S_i$. Therefore, we use the following posterior Q_i^α with hyperparameter α ,

$$Q_i^\alpha(S'_i, P)(h) = \frac{P(h) \exp(-\alpha \hat{L}(h, S'_i))}{Z_\alpha(S'_i, P)}.$$

Plugging into Eq.(6) (derivations in Appendix) yields that, with at least $1 - \delta$ probability,

$$R(Q, T) \leq \frac{1}{n} \sum_{i=1}^n \mathbb{E}_{P \sim \mathcal{Q}} \underbrace{\left[-\frac{1}{\beta} \log Z_\alpha(S'_i, P) + \hat{L}_{\frac{\Delta}{\beta}}(Q_i^\alpha, S_i, S'_i) \right]}_{W_2} + \tilde{\xi} D_{KL}(Q \| \mathcal{P}) + C. \quad (11)$$

where $\hat{L}_{\frac{\Delta}{\beta}}(Q_i^\alpha, S_i, S'_i) \triangleq \hat{L}(Q_i^\alpha, S_i) - \frac{\alpha}{\beta} \hat{L}(Q_i^\alpha, S'_i)$. We refer to the RHS of this equation as the PACMAML objective, because Eq.(11) comes from the PAC-Bayesian bound of Eq.(6), which is similar to MAML in subsampling the training data for base-learners.

Given these two objectives, the next step is to estimate the gradients of W_1 and W_2 , which can then be plugged into Monte-Carlo methods for estimating a hyper-posterior distribution of \mathcal{Q} (or optimization methods for finding an MAP solution).

Gradient Estimation In W_1 and W_2 , the terms $Z_\beta, Z_\alpha, \hat{L}_{\frac{\Delta}{\beta}}(Q_i^\alpha, S_i, S'_i)$ all involve integrations over h . When $P(h)$ is Gaussian and $\hat{L}(h, S_i)$ is a squared loss, such integrations have closed form solutions and the gradients can be analytically obtained. However, when $\hat{L}(h, S_i)$ is not a squared loss (such as the softmax loss), the integration does not have a closed form solution and we resort to

[‡]A slight difference is that MAML usually assumes $S_i \cap S'_i = \emptyset$; while in our setting, we assume $S'_i \subset S_i$. However, Theorem 4 still holds when $S_i \cap S'_i = \emptyset$.

approximations. For example, Rothfuss et al. [2020] directly approximates the objective W_1 with Monte-Carlo sampling, which however results in a biased gradient estimator.

Here, we follow an alternative approach from the REINFORCE algorithm [Williams, 1992], which instead approximates *the gradient of the objective* with Monte-Carlo methods, and has the benefit that the resulting gradient estimator is unbiased. Assuming that the model hypothesis h is parameterized by \mathbf{v} such that $\hat{L}(h, S_i) \triangleq \hat{L}(\mathbf{v}, S_i)$, and \mathbf{v} has prior $P(\mathbf{v}) = \mathcal{N}(\mathbf{v} | \mathbf{p}, \sigma^2)$ with meta-parameter \mathbf{p} , then

$$\log Z_\beta(S_i, \mathbf{p}) = \log \int \mathcal{N}(\mathbf{v} | \mathbf{p}, \sigma^2) \exp(-\beta \hat{L}(\mathbf{v}, S_i)) d\mathbf{v}.$$

Note that \mathbf{p} appears in the probability distribution $\mathcal{N}(\mathbf{v} | \mathbf{p}, \sigma^2)$ of the expectation, and the naive Monte-Carlo estimator of the gradient w.r.t. \mathbf{p} is known to exhibit high variance. To reduce the variance, we apply the reparameterization trick [Kingma and Welling, 2013] and rewrite $\mathbf{v} = \mathbf{p} + \mathbf{w}$ with $\mathbf{w} \sim \mathcal{N}(\mathbf{w} | \mathbf{0}, \sigma^2)$. This leads to the following gradient of W_1 ,

$$\frac{dW_1}{d\mathbf{p}} = -\frac{1}{\beta} \frac{d}{d\mathbf{p}} \log Z_\beta(S_i, \mathbf{p}) = \int Q_i^\beta(\mathbf{w}; S_i) \frac{\partial \hat{L}(\mathbf{p} + \mathbf{w}, S_i)}{\partial \mathbf{p}} d\mathbf{w}, \quad (12)$$

$$\text{where, } Q_i^\beta(\mathbf{w}; S_i) \propto \mathcal{N}(\mathbf{w} | \mathbf{0}, \sigma^2) \exp(-\beta \hat{L}(\mathbf{p} + \mathbf{w}, S_i)).$$

As for W_2 , we also need to evaluate the gradient of $\hat{L}_{\frac{\Delta}{\beta}}(Q_i^\alpha, S_i, S'_i)$, where

$$\frac{d}{d\mathbf{p}} \hat{L}_{\frac{\Delta}{\beta}}(Q_i^\alpha, S_i, S'_i) = \int Q_i^\alpha(\mathbf{w}; S'_i) \frac{\partial \hat{L}_{\frac{\Delta}{\beta}}(\mathbf{p} + \mathbf{w}, S_i, S'_i)}{\partial \mathbf{p}} d\mathbf{w} + \int \frac{\partial Q_i^\alpha(\mathbf{w}; S'_i)}{\partial \mathbf{p}} \hat{L}_{\frac{\Delta}{\beta}}(\mathbf{p} + \mathbf{w}, S_i, S'_i) d\mathbf{w}. \quad (13)$$

The first term of Eq.(13) is similar to the gradient in Eq.(12). The Monte-Carlo gradient estimator of the second term, however, exhibits the same high-variance problem as in the policy gradient method. As a remedy, we approximate the gradient with the one from the Softmax Policy Gradient [Ding and Soricut, 2017], which yields a low-variance approximate gradient of W_2 (details in Appendix):

$$\frac{dW_2}{d\mathbf{p}} \simeq \int Q_i^\alpha(\mathbf{w}; S'_i) \frac{\partial \hat{L}(\mathbf{p} + \mathbf{w}; S_i)}{\partial \mathbf{p}} d\mathbf{w} + \frac{\alpha}{\beta} \int (Q_i^\beta(\mathbf{w}; S_i) - Q_i^\alpha(\mathbf{w}; S'_i)) \frac{\partial \hat{L}(\mathbf{p} + \mathbf{w}; S'_i)}{\partial \mathbf{p}} d\mathbf{w}. \quad (14)$$

The first-term in Eq.(14) is similar to the gradient of the First-order MAML (FOMAML, Finn et al. [2017]). The second term involves Q_i^β and Q_i^α , which are similar to the leader and the chaser in BMAML [Yoon et al., 2018]. Intuitively, the second term provides additional information that plays a similar role to the high-order derivatives in MAML. However, unlike MAML and BMAML, Eq.(14) only involves partial derivatives over \mathbf{p} (since \mathbf{w} is not a function of \mathbf{p}) and therefore relies only on first-order derivatives which contribute to its efficiency and stability.

To estimate Eq.(12) and Eq.(14) in practice, we first draw samples $\mathbf{w}_{(n)}^\alpha \sim Q_i^\alpha(\mathbf{w}; S'_i)$ and $\mathbf{w}_{(n)}^\beta \sim Q_i^\beta(\mathbf{w}; S_i)$ using the Monte-Carlo sampling (e.g. SGLD [Welling and Teh, 2011] or SVGD [Liu and Wang, 2016]). After plugging the samples into $\hat{L}(\mathbf{p} + \mathbf{w}; S_i)$ and $\hat{L}(\mathbf{p} + \mathbf{w}; S'_i)$, we can apply automatic gradient computations (with Tensorflow [Abadi et al., 2015] or Pytorch [Paszke et al., 2019]) over \mathbf{p} to get the stochastic gradient estimator of W_1 and W_2 .

5 Experiments

In this section, we evaluate the two PAC-Bayesian algorithms as they were derived in the previous section: PACOH [Rothfuss et al., 2020] of Eq.(10) and PACMAML of Eq.(11). We use several few-shot learning benchmarks (both synthetic and real), and compare them against other existing meta-learning algorithms, including MAML [Finn et al., 2017], Reptile [Nichol et al., 2018], and BMAML [Yoon et al., 2018]. To fairly compare with other meta-learning algorithms that optimize a single model, we consider only the empirical Bayes method for PACOH and PACMAML, in which a single MAP solution of \mathcal{Q} is used, instead of Bayesian ensembles of \mathcal{Q} .

5.1 Few-Shot Regression Problem

Our first set of experiments are based on the synthetic regression environment setup from [Rothfuss et al., 2020], where the gradient can be obtained analytically. The base-learners $Q(S, P)$ are

modeled using Gaussian Process (GP) regression with a prior $P_\theta(h) = \mathcal{GP}(h|m_\theta(x), k_\theta(x, x'))$, where the mean function m_θ and the kernel function k_θ are instantiated as neural networks as in [Rothfuss et al., 2020]. For every example $z_j = (x_j, y_j)$ and a hypothesis h , the loss function is $l(h, z_j) = \|h(x_j) - y_j\|_2^2$ and the empirical risk is $\hat{L}(h, S_i) = \frac{1}{m_i} \sum_{j=1}^{m_i} l(h, z_j)$. The hyper-prior $\mathcal{P}(P_\theta) := \mathcal{P}(\theta) = \mathcal{N}(\theta|0, \sigma_0^2 I)$ is an isotropic Gaussian defined over the network parameters θ . The MAP approximated hyper-posterior takes the form of a delta function, where $\mathcal{Q}_{\theta_0}(P_\theta) := \mathcal{Q}_{\theta_0}(\theta) = \delta(\theta = \theta_0)$. As a result, we have that $D_{KL}(\mathcal{Q}_{\theta_0} \| \mathcal{P}) = \|\theta_0\|^2 / 2\sigma_0^2$, where we use $\sigma_0^2 = 3$ in our experiments.

We experiment with the synthetic *Sinusoid* environment (details in Appendix D.2), where we fix the number of observed tasks $n = 20$, and vary the number of examples per observed tasks from $m_i \in \{5, 10, 30, 50, 100\}$. The number of training examples for each target task is fixed to be $m = 5$, and another 100 examples for each target task are used as a test set to evaluate the generalization error. We report the averaged generalization error over 40 models, with the hyperparameters selected by 4-fold cross-validation over the 20 target tasks. Each model is trained on 1 of the 8 pre-sampled meta-training sets (each containing $n = 20$ observed tasks) and each set is run with 5 random seeds for network initialization. α and β are chosen based on the cross-validation from the grid $\beta/m_i \in \{10, 30, 100\}$, and $\alpha/m_i \in \{10, 20, 30, 40, 50, 60\}$.

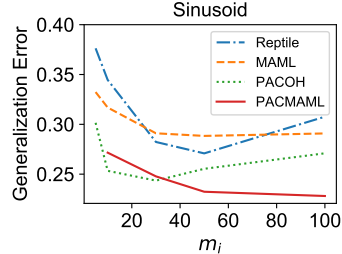


Figure 2: Generalization error (RMSE) on the Sinusoid dataset: PACMAML and MAML continue to improve as m_i increases.

Figure 2 shows the averaged generalization errors (RMSE) as m_i changes, for the Reptile (with optimal \mathbf{q}_i^*), MAML, PACOH, and PACMAML algorithms. The size of S'_i used for base-learner training in MAML and PACMAML is $m'_i = 5$ for all m_i . The hyperparameter values, the validation errors and the standard errors are reported in the Appendix D.3. As can be seen from the figure, the generalization errors of Reptile (blue) and PACOH (green), both derived from Theorem 3, have a U-shaped curve. That is, increasing the meta-training data m_i initially improves generalization in the few-shot target tasks, however, as m_i continues to grow well beyond m , generalization suffers. This confirms our conjecture from Theorem 3, that larger m_i has a mixed effect on its generalization behavior due to the penalty term Δ_λ . In contrast, the generalization error of MAML and PACMAML, both derived from Theorem 4, is monotonically decreasing as desired. Both the generalization error and the bound (in Fig.1) demonstrate that PACMAML is the most effective strategy of utilizing larger meta-training data for few-shot learning.

5.2 Few-shot Classification Problems

In addition to the regression problems where the gradients have closed-form, our next experiments evaluate how PACMAML perform on classification tasks using softmax losses with gradient estimators from Eq.(12) and Eq.(14). In order to fairly compare with MAML, which has only one set of inner adaptive parameters, we also only use one sample for approximating the inner posterior distribution \mathcal{Q}_i^α and \mathcal{Q}_i^β .

Image Classification Our first classification experiment is based on the miniImagenet classification task [Vinyals et al., 2016] involving a task adaptation of 5-way classification with a single training example per class (1-shot). The dataset consists of 60,000 color images of 84×84 dimension. The examples consist of total 100 classes that are partitioned into 64, 12, and 24 classes for meta-train, meta-validation, and meta-test, respectively. We generated the tasks following the same procedure as in [Finn et al., 2017] and used the same feature extraction model which contains 4 convolutional layers. Although the original MAML adapted the entire network in the inner loop, [Raghu et al., 2019] showed similar results by adapting only the top layer, which significantly reduced computational complexity. We follow the same "almost no inner loop" (ANIL) setting as [Raghu et al., 2019], and compare MAML with BMAML, PACOH and PACMAML. Reptile is not included, because it requires full model adaptation.

For all algorithms, we optimize for 6 steps in the inner loop to obtain the inner adaptive parameter (or a posterior sample \mathbf{w}). The data sizes of the observed tasks are varied from $m_i = \{10, 20, 40, 80\}$ and $m'_i = m = 5$ (one shot for each of 5 classes). We fixed $\alpha/\beta = m'_i/m_i$ and perform grid search

on α as well as the meta and inner learning rate on the meta-validation dataset. Other hyperparameters followed the setting in [Finn et al., 2017]. Further details are reported in the Appendix.

	FOMAML	MAML	BMAML	PACOH	PACMAML
$m_i = 10$	41.8 ± 0.9	47.3 ± 0.9	29.9 ± 0.9	31.2 ± 0.8	47.8 ± 0.9
$m_i = 20$	44.3 ± 0.9	48.0 ± 0.9	34.3 ± 0.9	37.0 ± 0.9	49.1 ± 0.9
$m_i = 40$	46.2 ± 1.0	47.8 ± 0.9	41.5 ± 0.9	41.6 ± 0.9	48.9 ± 0.9
$m_i = 80$	45.7 ± 0.9	48.1 ± 0.9	44.2 ± 0.9	44.6 ± 0.9	50.1 ± 0.9

Table 1: Averaged Generalization error and standard error in the ANIL setting.

The main meta-testing results are presented in Table 1. We find that PACOH performs significantly worse than PACMAML. One explanation for this is that in PACOH the base-learner (for top layer) is exposed to all S data, and may have already overfit on S and the meta-learner (for lower layers) is unable to learn further. The overfitting of the base-learner is more severe when m_i is small. Surprisingly, we find that BMAML behaves similarly poor in the ANIL 1-particle setting. In FOMAML, MAML and PACMAML, the base-learner is only trained on S' and the meta-learner can learn from the unseen examples in S and therefore no overfitting happens. Both MAML and PACMAML performs significantly better than FOMAML when m_i is small, but their performances saturate and improve little for larger m_i , which may due to the domain change between meta-training and testing (as the image class changes). Overall, PACMAML as a first-order method not only significantly outperforms FOMAML, but also marginally outperforms the high-order MAML, which demonstrates the effectiveness of PACMAML and its gradient estimator.

Natural Language Inference Lastly, we evaluate the meta-learning algorithms on the large-scale BERT-base [Devlin et al., 2019] model containing 110M parameters. Our experiment involves 12 practical natural language inference tasks from [Bansal et al., 2019] which include:[§] (1) entity typing: CoNLL-2003, MIT-Restaurant; (2) rating classification: the review ratings from the Amazon Reviews dataset in the domain of Books, DVD, Electronics, Kitchen; (3) text classification: social-media datasets from crowdflower that include Airline, Disaster, Emotion, Political Bias, Political Audience, Political Message.

Following [Bansal et al., 2019], we used the pretrained BERT-base model as our base model (hyperprior), and used GLUE benchmark tasks [Wang et al., 2018] for meta-training the models and meta-validation for hyperparameter search, before fine-tuning them for the 12 target tasks. The fine-tuning data contains $k \in \{4, 8, 16\}$ -shot data for each class in each task. For every k , 10 fine-tuning datasets were sampled for each target task. The final reported result is the average of the 10 models fine-tuned over these 10 datasets (for each task and each k separately), and evaluated on the entire test set for each target task [Bansal et al., 2019]. The data size of the observed tasks are fixed to be $m_i = 256$, where the data points for each observed task are randomly sampled from the training data of one of the GLUE tasks. Because the number of classes in these 12 few-shot tasks varies from 2 to 12, we choose the inner data size m'_i from $\{32, 64\}$ for MAML, BMAML and PACMAML. As in [Bansal et al., 2019], we also partition the set of model parameters to task-specific and task-agnostic. For the 12-layer BERT-base model, we consider a hyper-parameter $v \in \{6, 9, 11, 12\}$, where only the layers higher than the v -th layer are considered task-specific and will be adapted in the inner loop. When $v = 12$, only the top classification layers are adaptable. For BMAML, PACOH and PACMAML, we performed grid search on α and fixed $\alpha/\beta = m'_i/m_i$.

Due to space limitation, we only report the averaged generalization error over the 12 tasks in Table 2 (top). The detailed results of the 12 NLI tasks, their standard errors, as well as the hyperparameter selections are all included in the Appendix. We also include the SOTA results from [Bansal et al., 2020] for comparison and note that PACMAML is consistently the best performer over all three few-shot settings $k = 4, 8, 16$. In comparison, MAML and BMAML perform worse, possibly due to sensitivity to learning rates, as suggested by [Bansal et al., 2019]. Beyond generalization errors, in Table 2 (bottom) we also compare the memory usage of MAML/BMAML against PACMAML over different adaptive layer thresholds v . These results emphasize the computational advantage of PACMAML by showing that as more layers are adapted (lower v), MAML consumes significantly more memory due to its high-order derivatives.

[§]Data available at: <https://github.com/iesl/leopard>.

k	H-SMLMT [Bansal et al., 2020]	MAML	BMAML	PACOH	PACMAML
4	48.61	48.21	47.27	50.47	51.58
8	52.92	53.52	52.08	54.83	55.68
16	57.90	57.38	56.53	58.22	59.18
		$v=6$	$v=9$	$v=11$	$v=12$
	MAML	120G	57G	16G	4G
	BMAML	121G	59G	19G	4G
	PACMAML	33G	16G	8G	4G

Table 2: Top: Averaged Generalization error over the 12 NLI tasks. Bottom: The comparison of TPU memory (High Bandwidth Memory) usage with different adaptive layer thresholds v .

6 Discussion

We studied two PAC-Bayesian bounds for meta-learning in the few-shot case, where the number of examples in the target task is significantly smaller than that in the observed tasks. As opposed to previous bounds, our bound in Theorem 4 remains tight in this scenario. We instantiated these new bounds and related them to the Reptile and MAML algorithms and furthermore derived the PACMAML algorithm, and showed its efficiency and effectiveness over several meta-learning benchmarks. Broadly speaking, our work falls into the category of PAC-Bayesian theories of non-i.i.d data [Pentina and Lampert, 2015]; however, our study case is more specific and our bounds are based on practical strategies. One major limitation of the work is that we do not take into account a data domain shift (e.g. [Germain et al., 2016b]), which is often present in practice. However, the study of domain shift from a theoretical perspective requires additional assumptions and knowledge about the target data, which do not always exist in practice. We leave a deeper discussion and exploration on these topics to future work.

References

- M. Abadi, A. Agarwal, P. Barham, E. Brevdo, Z. Chen, C. Citro, G. S. Corrado, A. Davis, J. Dean, M. Devin, S. Ghemawat, I. Goodfellow, A. Harp, G. Irving, M. Isard, Y. Jia, R. Jozefowicz, L. Kaiser, M. Kudlur, J. Levenberg, D. Mané, R. Monga, S. Moore, D. Murray, C. Olah, M. Schuster, J. Shlens, B. Steiner, I. Sutskever, K. Talwar, P. Tucker, V. Vanhoucke, V. Vasudevan, F. Viégas, O. Vinyals, P. Warden, M. Wattenberg, M. Wicke, Y. Yu, and X. Zheng. TensorFlow: Large-scale machine learning on heterogeneous systems, 2015. URL <https://www.tensorflow.org/>. Software available from tensorflow.org.
- P. Alquier, J. Ridgway, and N. Chopin. On the properties of variational approximations of gibbs posteriors. *The Journal of Machine Learning Research*, 17(1):8374–8414, 2016.
- R. Amit and R. Meir. Meta-learning by adjusting priors based on extended PAC-Bayes theory. In J. Dy and A. Krause, editors, *Proceedings of the 35th International Conference on Machine Learning*, volume 80 of *Proceedings of Machine Learning Research*, pages 205–214, Stockholm, Sweden, 10–15 Jul 2018. PMLR.
- T. Bansal, R. Jha, and A. McCallum. Learning to few-shot learn across diverse natural language classification tasks. *arXiv preprint arXiv:1911.03863*, 2019.
- T. Bansal, R. Jha, T. Munkhdalai, and A. McCallum. Self-supervised meta-learning for few-shot natural language classification tasks. *arXiv preprint arXiv:2009.08445*, 2020.
- J. Baxter. Theoretical models of learning to learn. In *Learning to learn*, pages 71–94. Springer, 1998.
- J. Devlin, M.-W. Chang, K. Lee, and K. Toutanova. BERT: Pre-training of deep bidirectional transformers for language understanding. In *Proceedings of the 2019 Conference of the North American Chapter of the Association for Computational Linguistics: Human Language Technologies, Volume 1 (Long and Short Papers)*, June 2019.
- N. Ding and R. Soricut. Cold-start reinforcement learning with softmax policy gradient. In *Proceedings of the 31st International Conference on Neural Information Processing Systems*, pages 2814–2823, 2017.

- C. Finn, P. Abbeel, and S. Levine. Model-agnostic meta-learning for fast adaptation of deep networks. *arXiv preprint arXiv:1703.03400*, 2017.
- P. Germain, A. Lacasse, F. Laviolette, and M. Marchand. PAC-bayesian learning of linear classifiers. In *Proceedings of the 26th Annual International Conference on Machine Learning*, pages 353–360, 2009.
- P. Germain, F. Bach, A. Lacoste, and S. Lacoste-Julien. PAC-bayesian theory meets bayesian inference. *Advances in Neural Information Processing Systems*, 29:1884–1892, 2016a.
- P. Germain, A. Habrard, F. Laviolette, and E. Morvant. A new pac-bayesian perspective on domain adaptation. In *International conference on machine learning*, pages 859–868. PMLR, 2016b.
- D. P. Kingma and M. Welling. Auto-encoding variational bayes. *arXiv preprint arXiv:1312.6114*, 2013.
- Q. Liu and D. Wang. Stein variational gradient descent: A general purpose bayesian inference algorithm. *arXiv preprint arXiv:1608.04471*, 2016.
- D. A. McAllester. Some PAC-bayesian theorems. *Machine Learning*, 37(3):355–363, 1999.
- A. Nichol, J. Achiam, and J. Schulman. On first-order meta-learning algorithms. *arXiv preprint arXiv:1803.02999*, 2018.
- A. Paszke, S. Gross, F. Massa, A. Lerer, J. Bradbury, G. Chanan, T. Killeen, Z. Lin, N. Gimelshein, L. Antiga, A. Desmaison, A. Kopf, E. Yang, Z. DeVito, M. Raison, A. Tejani, S. Chilamkurthy, B. Steiner, L. Fang, J. Bai, and S. Chintala. Pytorch: An imperative style, high-performance deep learning library. In H. Wallach, H. Larochelle, A. Beygelzimer, F. d'Alché-Buc, E. Fox, and R. Garnett, editors, *Advances in Neural Information Processing Systems 32*, pages 8024–8035. Curran Associates, Inc., 2019. URL <http://papers.neurips.cc/paper/9015-pytorch-an-imperative-style-high-performance-deep-learning-library.pdf>.
- A. Pentina and C. H. Lampert. A pac-bayesian bound for lifelong learning. In *Proceedings of the 31st International Conference on International Conference on Machine Learning - Volume 32, ICML 14*, page II-991–II-999, 2014.
- A. Pentina and C. H. Lampert. Lifelong learning with non-iid tasks. *Advances in Neural Information Processing Systems*, 28:1540–1548, 2015.
- A. Raghu, M. Raghu, S. Bengio, and O. Vinyals. Rapid learning or feature reuse? towards understanding the effectiveness of maml. *arXiv preprint arXiv:1909.09157*, 2019.
- S. Ravi and H. Larochelle. Optimization as a model for few-shot learning. In *ICLR*, 2017.
- J. Rothfuss, V. Fortuin, and A. Krause. PACOH: Bayes-optimal meta-learning with pac-guarantees, 2020.
- O. Russakovsky, J. Deng, H. Su, J. Krause, S. Satheesh, S. Ma, Z. Huang, A. Karpathy, A. Khosla, M. Bernstein, et al. Imagenet large scale visual recognition challenge. *International journal of computer vision*, 115(3):211–252, 2015.
- N. Tripuraneni, M. I. Jordan, and C. Jin. On the theory of transfer learning: The importance of task diversity. *arXiv preprint arXiv:2006.11650*, 2020.
- O. Vinyals, C. Blundell, T. Lillicrap, K. Kavukcuoglu, and D. Wierstra. Matching networks for one shot learning. *arXiv preprint arXiv:1606.04080*, 2016.
- A. Wang, A. Singh, J. Michael, F. Hill, O. Levy, and S. R. Bowman. Glue: A multi-task benchmark and analysis platform for natural language understanding. *arXiv preprint arXiv:1804.07461*, 2018.
- M. Welling and Y. W. Teh. Bayesian learning via stochastic gradient langevin dynamics. In *Proceedings of the 28th international conference on machine learning (ICML-11)*, pages 681–688. Citeseer, 2011.

- R. J. Williams. Simple statistical gradient-following algorithms for connectionist reinforcement learning. In *Machine Learning*, pages 229–256, 1992.
- J. Yoon, T. Kim, O. Dia, S. Kim, Y. Bengio, and S. Ahn. Bayesian model-agnostic meta-learning. In *Proceedings of the 32nd International Conference on Neural Information Processing Systems*, pages 7343–7353, 2018.

A Proofs

In this section, we provide proofs of the main theorems presented in the paper. We also provide a brief overview of the proof of Theorem 2 from [Pentina and Lampert, 2015, Rothfuss et al., 2020], since the bound decomposition strategy will also be used in the new theorems of the paper.

A.1 Brief Proof of Theorem 2 [Pentina and Lampert, 2015, Rothfuss et al., 2020]

Given a task environment T and a set of n observed tasks $(D_i, m_i) \sim T$, let \mathcal{P} be a fixed hyper-prior and $\lambda > 0, \beta > 0$, with probability at least $1 - \delta$ over samples $S_1 \in D_1^{m_1}, \dots, S_n \in D_n^{m_n}$, we have for all base learner Q and all hyper-posterior \mathcal{Q} ,

$$\begin{aligned} R(\mathcal{Q}, T) &\leq \hat{R}(\mathcal{Q}, S_{i=1}^n) + \tilde{\xi} D_{KL}(\mathcal{Q} \| \mathcal{P}) \\ &\quad + \frac{1}{n\beta} \sum_{i=1}^n \mathbb{E}_{P \sim \mathcal{Q}} [D_{KL}(Q(S_i, P) \| P)] + C(\delta, \lambda, \beta, n, m_i), \end{aligned}$$

where $\tilde{\xi} = \frac{1}{\lambda} + \frac{1}{n\beta}$.

Proof The bound in Theorem 2 was proved by decomposing it into two components:

- "Task specific generalization bound", that bounds the generalization error averaged over all observed tasks τ_i :

$$\begin{aligned} &\mathbb{E}_{P \sim \mathcal{Q}} \left[\frac{1}{n} \sum_{i=1}^n L(Q(S_i, P), D_i) \right] \\ &\leq \hat{R}(\mathcal{Q}, S_{i=1}^n) + \frac{1}{n\beta} D_{KL}(\mathcal{Q} \| \mathcal{P}) + \frac{1}{n\beta} \sum_{i=1}^n \mathbb{E}_{P \sim \mathcal{Q}} [D_{KL}(Q(S_i, P) \| P)] \\ &\quad + \frac{1}{n\beta} \log \frac{1}{\delta} + \frac{1}{n} \sum_{i=1}^n \frac{m_i}{\beta} \Psi_1\left(\frac{\beta}{m_i}\right) \end{aligned} \quad (15)$$

where

$$\begin{aligned} \hat{R}(\mathcal{Q}, S_{i=1}^n) &= \mathbb{E}_{P \sim \mathcal{Q}} \left[\frac{1}{n} \sum_{i=1}^n \hat{L}(Q(S_i, P), S_i) \right], \\ \Psi_1(\beta) &= \log \mathbb{E}_{P \sim \mathcal{P}} \mathbb{E}_{h \sim P} \mathbb{E}_{z_{ij} \sim D_i} \left[e^{\beta(\mathbb{E}_{z_i \sim D_i} [l(h_i, z_i)] - l(h_i, z_{ij}))} \right]. \end{aligned}$$

- "Task environment generalization bound", that bounds the transfer error from the observed tasks to the new target tasks:

$$\begin{aligned} R(\mathcal{Q}, T) &\leq \frac{1}{n} \sum_{i=1}^n \mathbb{E}_{P \sim \mathcal{Q}} [L(Q(S_i, P), D_i)] \\ &\quad + \frac{1}{\lambda} \left(D_{KL}(\mathcal{Q} \| \mathcal{P}) + \log \frac{1}{\delta} \right) + \frac{n}{\lambda} \Psi_2\left(\frac{\lambda}{n}\right). \end{aligned} \quad (16)$$

where

$$\Psi_2(\lambda) = \log \mathbb{E}_{P \sim \mathcal{P}} \mathbb{E}_{D_i \sim T, S_i \sim D_i^{m_i}} \left[e^{\lambda(\mathbb{E}_{D_i \sim T, S_i \sim D_i^{m_i}} [R_{S_i}(P)] - R_{S_i}(P))} \right].$$

Detailed proofs of these two generalization bounds can be found in the appendices of [Pentina and Lampert, 2015, Rothfuss et al., 2020]. Subsequently, combining Eq.(15) with Eq.(16), it is straightforward to get Eq.(4), with

$$C(\delta, \lambda, \beta, n, m_i) = \tilde{\xi} \log \frac{1}{\delta} + \frac{1}{n} \sum_{i=1}^n \frac{m_i}{\beta} \Psi_1\left(\frac{\beta}{m_i}\right) + \frac{n}{\lambda} \Psi_2\left(\frac{\lambda}{n}\right). \quad (17)$$

■

A.2 Proof of Theorem 3

For a target task environment T and an observed task environment \tilde{T} where $\mathbb{E}_{\tilde{T}}[D] = \mathbb{E}_T[D]$ and $\mathbb{E}_{\tilde{T}}[m] \geq \mathbb{E}_T[m]$, let \mathcal{P} be a fixed hyper-prior and $\lambda > 0$, $\beta > 0$, then with probability at least $1 - \delta$ over samples $S_1 \in D_1^{m_1}, \dots, S_n \in D_n^{m_n}$ where $(D_i, m_i) \sim \tilde{T}$, we have, for all base learners Q and hyper-posterior \mathcal{Q} ,

$$\begin{aligned} R(\mathcal{Q}, T) &\leq \hat{R}(\mathcal{Q}, S_{i=1}^n) + \tilde{\xi} D_{KL}(\mathcal{Q} \| \mathcal{P}) + \frac{1}{n\beta} \sum_{i=1}^n \mathbb{E}_{P \sim \mathcal{Q}} [D_{KL}(Q(S_i, P) \| P)] \\ &\quad + C(\delta, \lambda, \beta, n, m_i) + \Delta_\lambda(\mathcal{P}, T, \tilde{T}), \end{aligned}$$

where $\Delta_\lambda(\mathcal{P}, T, \tilde{T}) = \frac{1}{\lambda} \log \mathbb{E}_{P \in \mathcal{P}} e^{\lambda(R(P, T) - R(P, \tilde{T}))}$, and $\tilde{\xi} = \frac{1}{\lambda} + \frac{1}{n\beta}$.

Proof The "task specific generalization bound" has the same form as Eq.(15).

For the "task environment generalization bound", define the "meta-training" generalization error of a given prior P on the observed task $(D_1, m_1), \dots, (D_n, m_n) \sim \tilde{T}$ as

$$\begin{aligned} R_{S_{\tilde{T}}}(P) &\triangleq \frac{1}{n} \sum_{i=1}^n L(Q(S_i, P), D_i) \\ &= \frac{1}{n} \sum_{i=1}^n \mathbb{E}_{z_i \sim D_i} \mathbb{E}_{h_i \sim Q(h_i | P, S_i)} [L(h_i, z_i)], \end{aligned}$$

where $S_i \sim D_i^{m_i}$ and $S_{\tilde{T}} = \{S_1, \dots, S_n\}$. Similarly, the generalization error on the target task environment T is

$$R(P, T) = \mathbb{E}_{(D, m) \sim T} \mathbb{E}_{S \sim D^m} \mathbb{E}_{z \in D} \mathbb{E}_{h \sim Q(h | P, S)} [L(h, z)].$$

Using the Markov Inequality, with at least $1 - \delta$ probability,

$$\begin{aligned} &\mathbb{E}_{P \sim \mathcal{P}} \left[e^{\lambda(R(P, T) - R_{S_{\tilde{T}}}(P))} \right] \\ &\leq \frac{1}{\delta} \mathbb{E}_{P \sim \mathcal{P}} \mathbb{E}_{D_i \sim T, S_i \sim D_i^{m_i}}^{i=1, \dots, n} \left[e^{\lambda(R(P, T) - R_{S_{\tilde{T}}}(P))} \right]. \end{aligned}$$

The left-hand side can be lower bounded by,

$$\begin{aligned} &\log \mathbb{E}_{P \sim \mathcal{P}} \left[e^{\lambda(R(P, T) - R_{S_{\tilde{T}}}(P))} \right] \\ &= \log \mathbb{E}_{P \sim \mathcal{Q}} \frac{\mathcal{P}(P)}{\mathcal{Q}(P)} e^{\lambda(R(P, T) - R_{S_{\tilde{T}}}(P))} \\ &\geq \mathbb{E}_{P \sim \mathcal{Q}} \log \frac{\mathcal{P}(P)}{\mathcal{Q}(P)} + \lambda \mathbb{E}_{P \sim \mathcal{Q}} [R(P, T) - R_{S_{\tilde{T}}}(P)] \\ &= -D_{KL}(\mathcal{Q} \| \mathcal{P}) + \lambda(R(\mathcal{Q}, T) - \mathbb{E}_{P \sim \mathcal{Q}} [R_{S_{\tilde{T}}}(P)]). \end{aligned}$$

The right-hand side is upper bounded by

$$\begin{aligned} &\log \frac{1}{\delta} \mathbb{E}_{P \sim \mathcal{P}} \mathbb{E}_{D_i \sim T, S_i \sim D_i^{m_i}}^{i=1, \dots, n} \left[e^{\lambda(R(P, T) - R_{S_{\tilde{T}}}(P))} \right] \\ &= \log \frac{1}{\delta} + \log \mathbb{E}_{P \sim \mathcal{P}} \mathbb{E}_{D_i \sim T, S_i \sim D_i^{m_i}}^{i=1, \dots, n} \left[e^{\lambda(R(P, T) - R_{S_{\tilde{T}}}(P))} \right] \\ &= \log \frac{1}{\delta} + \log \mathbb{E}_{P \sim \mathcal{P}} \left[e^{\lambda(R(P, T) - \mathbb{E}_{S_{\tilde{T}} \sim \tilde{T}} [R_{S_{\tilde{T}}}(P)])} \right] \\ &\quad + \log \mathbb{E}_{P \sim \mathcal{P}} \mathbb{E}_{D_i \sim T, S_i \sim D_i^{m_i}}^{i=1, \dots, n} \left[e^{\lambda(\mathbb{E}_{S_{\tilde{T}}} [R_{S_{\tilde{T}}}(P)] - R_{S_{\tilde{T}}}(P))} \right] \\ &\leq \log \frac{1}{\delta} + \log \mathbb{E}_{P \sim \mathcal{P}} \left[e^{\lambda(R(P, T) - \mathbb{E}_{S_{\tilde{T}}} [R_{S_{\tilde{T}}}(P)])} \right] + n\Psi_2\left(\frac{\lambda}{n}\right), \end{aligned} \tag{18}$$

where,

$$\begin{aligned}
& \mathbb{E}_{S_{\tilde{T}}} [R_{S_{\tilde{T}}}(P)] \\
& \triangleq \mathbb{E}_{\substack{i=1, \dots, n \\ (D_i, m_i) \sim \tilde{T}, S_i \sim D_i^{m_i}}} [R_{S_{\tilde{T}}}(P)] \\
& = \frac{1}{n} \sum_{i=1}^n \mathbb{E}_{(D_i, m_i) \sim \tilde{T}} \mathbb{E}_{S_i \sim D_i^{m_i}} \mathbb{E}_{z_i \in D_i} \mathbb{E}_{h_i \sim Q(h_i | P, S_i)} [L(h_i, z_i)] \\
& = \mathbb{E}_{(D, m) \sim \tilde{T}} \mathbb{E}_{S \sim D^m} \mathbb{E}_{z \in D} \mathbb{E}_{h \sim Q(h | P, S)} [L(h, z)] \\
& = R(P, \tilde{T}).
\end{aligned}$$

Combining the left-hand and right-hand bounds together, we have with at least probability $1 - \delta$,

$$\begin{aligned}
R(\mathcal{Q}, T) & \leq \frac{1}{n} \sum_{i=1}^n \mathbb{E}_{P \sim \mathcal{Q}} [L(Q(S_i, P), D_i)] \\
& \quad + \frac{1}{\lambda} \left(D_{KL}(\mathcal{Q} \| \mathcal{P}) + \log \frac{1}{\delta} + n\Psi_2\left(\frac{\lambda}{n}\right) \right) \\
& \quad + \frac{1}{\lambda} \log \mathbb{E}_{P \in \mathcal{P}} e^{\lambda(R(P, T) - R(P, \tilde{T}))}. \tag{19}
\end{aligned}$$

Lastly, combining Eq.(19) with Eq.(15) yields Eq.(5). ■

Furthermore, from Theorem 3, it is straightforward to obtain the following corollary.

Corollary 5 *For a target task environment T and an observed task environment \tilde{T} where $\mathbb{E}_{\tilde{T}}[D] = \mathbb{E}_T[D]$ and $\mathbb{E}_{\tilde{T}}[m] \geq \mathbb{E}_T[m]$, let \mathcal{P} be a fixed hyper-prior and $\lambda > 0$, $\beta > 0$, then with probability at least $1 - \delta$ over samples $S_1 \in D_1^{m_1}, \dots, S_n \in D_n^{m_n}$ where $(D_i, m_i) \sim \tilde{T}$, we have, for all base learners Q and hyper-posterior \mathcal{Q} ,*

$$\begin{aligned}
R(\mathcal{Q}, T) & \leq \hat{R}(\mathcal{Q}, S_{i=1}^n) + \tilde{\xi} D_{KL}(\mathcal{Q} \| \mathcal{P}) + \frac{1}{n\beta} \sum_{i=1}^n \mathbb{E}_{P \sim \mathcal{Q}} [D_{KL}(Q(S_i, P) \| P)] \\
& \quad + C(\delta, \lambda, \beta, n, m_i) + \Delta_\lambda(\mathcal{P}, \mathcal{Q}, T, \tilde{T}), \tag{20}
\end{aligned}$$

where $\Delta_\lambda(\mathcal{P}, \mathcal{Q}, T, \tilde{T}) = \min \left\{ \frac{1}{\lambda} \log \mathbb{E}_{P \in \mathcal{P}} e^{\lambda(R(P, T) - R(P, \tilde{T}))}, R(\mathcal{Q}, T) - R(\mathcal{Q}, \tilde{T}) \right\}$, and $\tilde{\xi} = \frac{1}{\lambda} + \frac{1}{n\beta}$.

Proof Similar to (16), we have

$$\begin{aligned}
R(\mathcal{Q}, \tilde{T}) & \leq \frac{1}{n} \sum_{i=1}^n \mathbb{E}_{P \sim \mathcal{Q}} [L(Q(S_i, P), D_i)] \\
& \quad + \frac{1}{\lambda} \left(D_{KL}(\mathcal{Q} \| \mathcal{P}) + \log \frac{1}{\delta} + n\Psi_2\left(\frac{\lambda}{n}\right) \right).
\end{aligned}$$

A simple reorganization of the terms leads to,

$$\begin{aligned}
R(\mathcal{Q}, T) & \leq \frac{1}{n} \sum_{i=1}^n \mathbb{E}_{P \sim \mathcal{Q}} [L(Q(S_i, P), D_i)] \\
& \quad + \frac{1}{\lambda} \left(D_{KL}(\mathcal{Q} \| \mathcal{P}) + \log \frac{1}{\delta} + n\Psi_2\left(\frac{\lambda}{n}\right) \right) + (R(\mathcal{Q}, T) - R(\mathcal{Q}, \tilde{T})). \tag{21}
\end{aligned}$$

Combining Eq.(21) with Eq.(19) and Eq.(15) gives the bound in Eq.(20). ■

Note that although Eq.(20) gives a potentially tighter bound than Eq.(5), empirically it makes little difference because $R(\mathcal{Q}, T) - R(\mathcal{Q}, \tilde{T})$ is inestimable in practice and cannot be directly optimized as a function of \mathcal{Q} . We will only numerically estimate its value in synthetic datasets in order to estimate the bound.

A.3 Proof of Theorem 4

For a target task environment T and an observed task environment \tilde{T} where $\mathbb{E}_{\tilde{T}}[D] = \mathbb{E}_T[D]$ and $\mathbb{E}_{\tilde{T}}[m] \geq \mathbb{E}_T[m]$, let \mathcal{P} be a fixed hyper-prior and $\lambda > 0$, $\beta > 0$, then with probability at least $1 - \delta$ over samples $S_1 \in D_1^{m_1}, \dots, S_n \in D_n^{m_n}$ where $(D_i, m_i) \sim \tilde{T}$, and subsamples $S'_1 \in D_1^{m'_1} \subset S_1, \dots, S'_n \in D_n^{m'_n} \subset S_n$, where $\mathbb{E}[m'_i] = \mathbb{E}_T[m]$, we have, for all base learner Q and all hyper-posterior \mathcal{Q} ,

$$R(\mathcal{Q}, T) \leq \mathbb{E}_{P \sim \mathcal{Q}} \left[\frac{1}{n} \sum_{i=1}^n \hat{L}(Q(S'_i, P), S_i) \right] + \tilde{\xi} D_{KL}(\mathcal{Q} \| \mathcal{P}) + \frac{1}{n\beta} \sum_{i=1}^n \mathbb{E}_{P \sim \mathcal{Q}} [D_{KL}(Q(S'_i, P) \| P)] + C(\delta, \lambda, \beta, n, m_i),$$

where $\tilde{\xi} = \frac{1}{\lambda} + \frac{1}{n\beta}$.

Proof The "task environment generalization bound" is the same as the one in Theorem 2, because the base-learner in observed and target task have the same task environment T . Therefore, we have

$$R(\mathcal{Q}, T) \leq \frac{1}{n} \sum_{i=1}^n \mathbb{E}_{P \sim \mathcal{Q}} [L(Q(S'_i, P), D_i)] + \frac{1}{\lambda} \left(D_{KL}(\mathcal{Q} \| \mathcal{P}) + \log \frac{1}{\delta} \right) + \frac{n}{\lambda} \Psi_2\left(\frac{\lambda}{n}\right). \quad (22)$$

As for the "task-specific generalization bound", define,

$$\hat{L}(\mathbf{h}) = \frac{1}{n} \sum_{i=1}^n \frac{1}{m_i} \sum_{j=1}^{m_i} l(h_i, z_{ij}), \quad L(\mathbf{h}) = \frac{1}{n} \sum_{i=1}^n \mathbb{E}_{z_i \sim D_i} l(h_i, z_i),$$

where $z_{ij} \in S_i$ which is sampled from D_i . According to the Markov inequality, with at least $1 - \delta$ probability, we have

$$\mathbb{E}_{P \sim \mathcal{P}} \mathbb{E}_{\mathbf{h} \sim P^n} \left[e^{n\beta(L(\mathbf{h}) - \hat{L}(\mathbf{h}))} \right] \leq \frac{1}{\delta} \mathbb{E}_{P \sim \mathcal{P}} \mathbb{E}_{\mathbf{h} \sim P^n} \mathbb{E}_{\mathbf{S} \sim \mathbf{D}^m} \left[e^{n\beta(L(\mathbf{h}) - \hat{L}(\mathbf{h}))} \right]$$

Now take the logarithm of both sides, and transform the expectation over \mathcal{P}, P to \mathcal{Q}, Q , where we use base-learner $Q(S'_i, P)$ with $S'_i \in D_i^{m'_i}$. Then the LHS becomes

$$\begin{aligned} & \log \mathbb{E}_{P \sim \mathcal{P}} \mathbb{E}_{\mathbf{h} \sim P^n} \left[e^{n\beta(L(\mathbf{h}) - \hat{L}(\mathbf{h}))} \right] \\ &= \log \mathbb{E}_{P \sim \mathcal{Q}} \mathbb{E}_{\mathbf{h} \sim \mathbf{Q}(S', P)} \left[\frac{\mathcal{P}(P) \prod_{i=1}^n P(h_i)}{\mathcal{Q}(P) \prod_{i=1}^n Q_i(h_i | S'_i, P)} e^{n\beta(L(\mathbf{h}) - \hat{L}(\mathbf{h}))} \right] \\ &\geq -D_{KL}(\mathcal{Q} \| \mathcal{P}) - \sum_{i=1}^n \mathbb{E}_{P \sim \mathcal{Q}} [D_{KL}(Q(S'_i, P) \| P)] \\ &\quad + \beta \mathbb{E}_{P \sim \mathcal{Q}} \left[\sum_{i=1}^n L(Q(S'_i, P), D_i) \right] - \beta \mathbb{E}_{P \sim \mathcal{Q}} \left[\sum_{i=1}^n \hat{L}(Q(S'_i, P), S_i) \right]. \end{aligned}$$

The first equation uses the fact that the hyper-prior \mathcal{P} and hyper-posterior \mathcal{Q} as well as the prior P are shared across all n observed tasks. The inequality uses Jensen's inequality to move the logarithm inside expectation.

The RHS is

$$\begin{aligned} & \log \frac{1}{\delta} + \log \mathbb{E}_{P \sim \mathcal{P}} \mathbb{E}_{\mathbf{h} \sim P^n} \mathbb{E}_{\mathbf{S} \sim \mathbf{D}^m} \left[e^{n\beta(L(\mathbf{h}) - \hat{L}(\mathbf{h}))} \right] \\ &= \log \frac{1}{\delta} + \log \mathbb{E}_{P \sim \mathcal{P}} \mathbb{E}_{\mathbf{h} \sim P^n} \prod_{i=1}^n \prod_{j=1}^{m_i} \mathbb{E}_{z_{ij} \sim D_i} \left[e^{\frac{\beta}{m_i} (\mathbb{E}_{z_i \sim D_i} [l(h_i, z_i)] - l(h_i, z_{ij}))} \right] \\ &= \log \frac{1}{\delta} + \sum_{i=1}^n m_i \Psi_1\left(\frac{\beta}{m_i}\right). \end{aligned}$$

Now, combining the LHS and RHS together, we get that with at least $1 - \delta$ probability,

$$\begin{aligned}
& \mathbb{E}_{P \sim \mathcal{Q}} \left[\frac{1}{n} \sum_{i=1}^n L(Q(S'_i, P), D_i) \right] \\
& \leq \mathbb{E}_{P \sim \mathcal{Q}} \left[\frac{1}{n} \sum_{i=1}^n L(Q(S'_i, P), S_i) \right] + \frac{1}{n\beta} D_{KL}(\mathcal{Q} \parallel \mathcal{P}) + \frac{1}{n\beta} \sum_{i=1}^n \mathbb{E}_{P \sim \mathcal{Q}} [D_{KL}(Q(S'_i, P) \parallel P)] \\
& \quad + \frac{1}{n\beta} \log \frac{1}{\delta} + \frac{1}{n} \sum_{i=1}^n \frac{m_i}{\beta} \Psi_1\left(\frac{\beta}{m_i}\right). \tag{23}
\end{aligned}$$

Combining Eq.(22) with Eq.(23) immediately yields Eq.(6). \blacksquare

B Derivations of MAML and Reptile

In this section, we derive a couple of meta-learning algorithms based on the MAP estimation of PAC-Bayesian bounds. To this end, we assume that the distribution families of the hyper-posterior $\mathcal{Q}(P)$ and posterior $Q_i(h)$ are from delta functions. In addition, we use the isotropic Gaussian priors for the hyper-prior $\mathcal{P}(P)$ and the prior $P(h)$ on all model parameters,

$$\begin{aligned}
\mathcal{P}(P) &= \mathcal{N}(\mathbf{p} \mid 0, \sigma_0^2) \\
\mathcal{Q}(P) &= \delta(\mathbf{p} = \mathbf{p}_0) \\
P(h) &= \mathcal{N}(\mathbf{h} \mid \mathbf{p}, \sigma^2) \\
Q_i(h) &= \delta(\mathbf{h} = \mathbf{q}_i) \quad \forall i = 1, \dots, n.
\end{aligned}$$

This way we have a closed form solution for the two KL terms, which are (up to a constant)

$$\begin{aligned}
D_{KL}(\mathcal{Q} \parallel \mathcal{P}) &= \int d\mathbf{p} \delta(\mathbf{p} = \mathbf{p}_0) \cdot \left(\frac{\|\mathbf{p}\|^2}{2\sigma_0^2} + \frac{k}{2} \log(2\pi\sigma_0^2) + \log \delta(\mathbf{p} = \mathbf{p}_0) \right) \\
&= \frac{\|\mathbf{p}_0\|^2}{2\sigma_0^2} + \frac{k}{2} \log(2\pi\sigma_0^2) + c,
\end{aligned}$$

where k is the dimension of \mathbf{p} and c is a constant. Similarly,

$$\begin{aligned}
& \mathbb{E}_{P \sim \mathcal{Q}} [D_{KL}(Q_i \mid P)] \\
&= \int d\mathbf{p} \delta(\mathbf{p} = \mathbf{p}_0) \int d\mathbf{h} \delta(\mathbf{h} = \mathbf{q}_i) \cdot \left(\frac{\|\mathbf{h} - \mathbf{p}\|^2}{2\sigma^2} + \frac{k}{2} \log(2\pi\sigma^2) + \log \delta(\mathbf{h} = \mathbf{q}_i) \right) \\
&= \int d\mathbf{p} \delta(\mathbf{p} = \mathbf{p}_0) \cdot \frac{\|\mathbf{p} - \mathbf{q}_i\|^2}{2\sigma^2} + \frac{k}{2} \log(2\pi\sigma^2) + c \\
&= \frac{\|\mathbf{p}_0 - \mathbf{q}_i\|^2}{2\sigma^2} + \frac{k}{2} \log(2\pi\sigma^2) + c.
\end{aligned}$$

Plugging in the above results, the PAC-Bayesian bound ($PacB$) in Eq.(5) and Eq.(6) are both of the form of,

$$PacB = \frac{1}{n} \sum_{i=1}^n L(\mathbf{q}_i, S_i) + \frac{\tilde{\xi} \|\mathbf{p}_0\|^2}{2\sigma_0^2} + \frac{1}{n\beta} \sum_{i=1}^n \frac{\|\mathbf{p}_0 - \mathbf{q}_i\|^2}{2\sigma^2} + C',$$

where the constant C' corresponding to Eq.(5) and Eq.(6) are different by Δ_λ . The only free variable of $PacB$ is \mathbf{p}_0 . The base-learner \mathbf{q}_i can be any function of \mathbf{p}_0 and S_i for Eq.(5) or S'_i for Eq.(6). One could find the MAP estimation of $PacB$ by gradient descent with respect to \mathbf{p}_0 .

Note that in Eq.(5), for a given \mathbf{p}_0 and S_i , there exists an optimal base-learner \mathbf{q}_i^* in the form of,

$$\mathbf{q}_i^* = \underset{\mathbf{q}_i}{\operatorname{argmin}} (PacB) = \underset{\mathbf{q}_i}{\operatorname{argmin}} \left[L(\mathbf{q}_i, S_i) + \frac{\|\mathbf{p}_0 - \mathbf{q}_i\|^2}{2\beta\sigma^2} \right].$$

Given the optimal \mathbf{q}_i^* , the full derivative of $PacB$ with respect to \mathbf{p}_0 is substantially simpler,

$$\begin{aligned} \frac{d(PacB)}{d\mathbf{p}_0} &= \frac{\partial(PacB)}{\partial\mathbf{p}_0} + \left\langle \frac{\partial\mathbf{q}_i^*}{\partial\mathbf{p}_0}, \frac{\partial(PacB)}{\partial\mathbf{q}_i^*} \right\rangle \\ &= \frac{\partial(PacB)}{\partial\mathbf{p}_0} = \frac{\tilde{\xi}\mathbf{p}_0}{\sigma_0^2} + \frac{1}{n} \sum_{i=1}^n \frac{\mathbf{p}_0 - \mathbf{q}_i^*}{\beta\sigma^2}, \end{aligned} \quad (24)$$

where the 2nd equation is because $\frac{\partial(PacB)}{\partial\mathbf{q}_i^*} = 0$ for the optimal base-learner \mathbf{q}_i^* . Eq.(24) is the equivalent to the meta-update of the Reptile algorithm [Nichol et al., 2018], except that Reptile does not solve for the optimal base learner \mathbf{q}_i^* .

From the optimal condition, the base-learner \mathbf{q}_i^* satisfies,

$$\frac{\mathbf{p}_0 - \mathbf{q}_i^*}{\beta\sigma^2} = \nabla_{\mathbf{q}_i^*} L(\mathbf{q}_i^*, S_i).$$

Therefore, we can rewrite Eq.(24) in the form of the *implicit gradient*,

$$\frac{d(PacB)}{d\mathbf{p}_0} = \frac{\tilde{\xi}\mathbf{p}_0}{\sigma_0^2} + \frac{1}{n} \sum_{i=1}^n \nabla_{\mathbf{q}_i^*} L(\mathbf{q}_i^*, S_i).$$

In contrast, the standard multi-task objective uses the *explicit gradient*, where $\mathbf{q}_i = \mathbf{p}_0$ and

$$\frac{d(PacB)}{d\mathbf{p}_0} = \frac{\tilde{\xi}\mathbf{p}_0}{\sigma_0^2} + \frac{1}{n} \sum_{i=1}^n \nabla_{\mathbf{p}_0} L(\mathbf{p}_0, S_i).$$

C Derivations of PACMAML

For Theorem 4, we use the following posterior as the base-learner for observed task τ_i ,

$$Q_i(S'_i, P)(h) = \frac{P(h) \exp(-\alpha \hat{L}(h, S'_i))}{Z_\alpha(S'_i, P)}.$$

Plugging this Q_i into Eq.(6), we have

$$\begin{aligned} &R(\mathcal{Q}, T) \\ &\leq \mathbb{E}_{P \sim \mathcal{Q}} \left[\frac{1}{n} \sum_{i=1}^n \hat{L}(Q_i, S_i) \right] + \tilde{\xi} D_{KL}(\mathcal{Q} \| \mathcal{P}) + \frac{1}{n\beta} \sum_{i=1}^n \mathbb{E}_{P \sim \mathcal{Q}} [D_{KL}(Q_i \| P)] + C \\ &= \frac{1}{n} \sum_{i=1}^n \mathbb{E}_{P \sim \mathcal{Q}} \left[\hat{L}(Q_i, S_i) + \frac{1}{\beta} D_{KL}(Q_i \| P) \right] + \tilde{\xi} D_{KL}(\mathcal{Q} \| \mathcal{P}) + C \\ &= \frac{1}{n} \sum_{i=1}^n \mathbb{E}_{P \sim \mathcal{Q}} \mathbb{E}_{h \sim Q_i} \left[\hat{L}(h, S_i) + \frac{1}{\beta} \log Q_i(h) - \frac{1}{\beta} \log P(h) \right] + \tilde{\xi} D_{KL}(\mathcal{Q} \| \mathcal{P}) + C \\ &= \frac{1}{n} \sum_{i=1}^n \mathbb{E}_{P \sim \mathcal{Q}} \mathbb{E}_{h \sim Q_i} \left[\hat{L}(h, S_i) - \frac{\alpha}{\beta} \hat{L}(h, S'_i) - \frac{1}{\beta} \log Z_\alpha(S'_i, P) \right] + \tilde{\xi} D_{KL}(\mathcal{Q} \| \mathcal{P}) + C \\ &= \frac{1}{n} \sum_{i=1}^n \mathbb{E}_{P \sim \mathcal{Q}} \left[-\frac{1}{\beta} \log Z_\alpha(S'_i, P) + \hat{L}(Q_i, S_i) - \frac{\alpha}{\beta} \hat{L}(Q_i, S'_i) \right] + \tilde{\xi} D_{KL}(\mathcal{Q} \| \mathcal{P}) + C. \end{aligned}$$

where $C = \tilde{\xi} \log \frac{2}{\delta} + \frac{n}{\lambda} \Psi(\frac{\lambda}{n}) + \frac{1}{n} \sum_{i=1}^n \frac{m_i}{\beta} \Psi(\frac{\beta}{m_i})$.

C.1 The Gradient Estimator of PACOH and PACMAML

Assuming that the model hypothesis h is parameterized by \mathbf{v} such that $\hat{L}(h, S_i) \triangleq \hat{L}(\mathbf{v}, S_i)$, and \mathbf{v} has prior $P(\mathbf{v}) = \mathcal{N}(\mathbf{v} | \mathbf{p}, \sigma^2)$ with meta-parameter \mathbf{p} , then

$$\log Z_\beta(S_i, \mathbf{p}) = \log \int \mathcal{N}(\mathbf{v} | \mathbf{p}, \sigma^2) \exp(-\beta \hat{L}(\mathbf{v}, S_i)) d\mathbf{v}.$$

Note that the parameter \mathbf{p} appears in the probability distribution of the expectation, and the naive Monte-Carlo gradient estimator of such gradient is known to exhibit high variance. To reduce the variance, we apply the reparameterization trick [Kingma and Welling, 2013] and rewrite $\mathbf{v} = \mathbf{p} + \mathbf{w}$ with $\mathbf{w} \sim \mathcal{N}(\mathbf{w} | \mathbf{0}, \sigma^2)$, then

$$\log Z_\beta(S_i, \mathbf{p}) = \log \int \mathcal{N}(\mathbf{w} | \mathbf{0}, \sigma^2) \exp(-\beta \hat{L}(\mathbf{p} + \mathbf{w}, S_i)) d\mathbf{w}.$$

This leads to the gradient of W_1 in the following form,

$$\begin{aligned} \frac{d}{d\mathbf{p}} W_1 &= -\frac{1}{\beta} \frac{d}{d\mathbf{p}} \log Z_\beta(S_i, \mathbf{p}) = \int Q_i^\beta(\mathbf{w}; S_i) \frac{\partial \hat{L}(\mathbf{p} + \mathbf{w}, S_i)}{\partial \mathbf{p}} d\mathbf{w}, \\ \text{where, } Q_i^\beta(\mathbf{w}; S_i) &\propto \mathcal{N}(\mathbf{w} | \mathbf{0}, \sigma^2) \exp(-\beta \hat{L}(\mathbf{p} + \mathbf{w}, S_i)). \end{aligned}$$

As for W_2 , the first term is similar to W_1 , but we also need to evaluate the gradient of $\hat{L}_{\frac{\Delta}{\beta}}(Q_i^\alpha, S_i, S'_i)$, which is

$$\frac{d}{d\mathbf{p}} \hat{L}_{\frac{\Delta}{\beta}}(Q_i^\alpha, S_i, S'_i) = \int Q_i^\alpha(\mathbf{w}; S'_i) \frac{\partial \hat{L}_{\frac{\Delta}{\beta}}(\mathbf{p} + \mathbf{w}, S_i, S'_i)}{\partial \mathbf{p}} d\mathbf{w} + \int \frac{\partial Q_i^\alpha(\mathbf{w}; S'_i)}{\partial \mathbf{p}} \hat{L}_{\frac{\Delta}{\beta}}(\mathbf{p} + \mathbf{w}, S_i, S'_i) d\mathbf{w}. \quad (25)$$

The second term of Eq.(25) is equivalent to,

$$\begin{aligned} &\int \frac{\partial Q_i^\alpha(\mathbf{w}; S'_i)}{\partial \mathbf{p}} \hat{L}_{\frac{\Delta}{\beta}}(\mathbf{p} + \mathbf{w}, S_i, S'_i) d\mathbf{w} \\ &= -\frac{1}{\beta} \frac{\partial}{\partial \mathbf{p}} \int Q_i^\alpha(\mathbf{w}; S'_i) \text{stop_grad} \left(-\beta \hat{L}_{\frac{\Delta}{\beta}}(\mathbf{p} + \mathbf{w}, S_i, S'_i) \right) d\mathbf{w}. \end{aligned}$$

The Monte-Carlo gradient estimator of this has the same high-variance problem as in the policy gradient method, which causes unreliable inference without warm-start. Instead, we apply the cold-start policy gradient method by approximating the loss with the one from the softmax value function [Ding and Soricut, 2017] as follows,

$$\begin{aligned} &-\frac{1}{\beta} \int Q_i^\alpha(\mathbf{w}; S'_i) \text{stop_grad} \left(-\beta \hat{L}_{\frac{\Delta}{\beta}}(\mathbf{p} + \mathbf{w}, S_i, S'_i) \right) d\mathbf{w} \\ &\geq -\frac{1}{\beta} \log \int Q_i^\alpha(\mathbf{w}; S'_i) \exp \left(\text{stop_grad} \left(-\beta \hat{L}_{\frac{\Delta}{\beta}}(\mathbf{p} + \mathbf{w}, S_i, S'_i) \right) \right) d\mathbf{w}. \end{aligned}$$

Then we take the gradient of the softmax value function,

$$\begin{aligned} &-\frac{1}{\beta} \frac{\partial}{\partial \mathbf{p}} \log \int Q_i^\alpha(\mathbf{w}; S'_i) \exp \left(\text{stop_grad} \left(-\beta \hat{L}_{\frac{\Delta}{\beta}}(\mathbf{p} + \mathbf{w}, S_i, S'_i) \right) \right) d\mathbf{w} \\ &= -\frac{1}{\beta} \int Q_i^\beta(\mathbf{w}; S_i) \frac{\partial \log Q_i^\alpha(\mathbf{w}; S'_i)}{\partial \mathbf{p}} d\mathbf{w} \\ &= \frac{\alpha}{\beta} \int \left(Q_i^\beta(\mathbf{w}; S_i) - Q_i^\alpha(\mathbf{w}; S'_i) \right) \frac{\partial \hat{L}(\mathbf{p} + \mathbf{w}, S'_i)}{\partial \mathbf{p}} d\mathbf{w}. \end{aligned}$$

This yields the overall gradient of W_2 to be,

$$\begin{aligned} \frac{d}{d\mathbf{p}} W_2 &\simeq \frac{\alpha}{\beta} \int Q_i^\beta(\mathbf{w}; S_i) \frac{\partial \hat{L}(\mathbf{p} + \mathbf{w}; S'_i)}{\partial \mathbf{p}} d\mathbf{w} + \int Q_i^\alpha(\mathbf{w}; S'_i) \frac{\partial \hat{L}_{\frac{\Delta}{\beta}}(\mathbf{p} + \mathbf{w}, S_i, S'_i)}{\partial \mathbf{p}} d\mathbf{w} \\ &= \int Q_i^\alpha(\mathbf{w}; S'_i) \frac{\partial \hat{L}(\mathbf{p} + \mathbf{w}; S_i)}{\partial \mathbf{p}} d\mathbf{w} + \frac{\alpha}{\beta} \int \left(Q_i^\beta(\mathbf{w}; S_i) - Q_i^\alpha(\mathbf{w}; S'_i) \right) \frac{\partial \hat{L}(\mathbf{p} + \mathbf{w}; S'_i)}{\partial \mathbf{p}} d\mathbf{w}. \end{aligned}$$

D Experiment Details of the Regression Problem

D.1 Gaussian Process Model Details

We use the Gaussian process prior, where $P_\theta(h) = \mathcal{GP}(h | m_\theta(x), k_\theta(x, x'))$ and $k_\theta(x, x') = \frac{1}{2} \exp(-\|\phi_\theta(x) - \phi_\theta(x')\|^2)$. Both $m_\theta(x)$ and $\phi_\theta(x)$ are instantiated to be neural networks. The

networks are composed of an input layer of size 1×32 , a hidden layer of size 32×32 . m_θ and ϕ_θ has an output layer of size 32×1 and 32×2 , respectively.

We focused on regression problems where for every example $z_j = (x_j, y_j)$ and a hypothesis h , the l_2 -loss function is used so that $l(h, z_j) = \|h(x_j) - y_j\|_2^2$. This leads to a Gaussian likelihood function. Assuming there are m examples in the dataset, we have

$$\begin{aligned} P(y|h, x) &= \mathcal{N}\left(h, \frac{m}{2\alpha}I\right) \\ &= \frac{1}{(\pi m/\alpha)^{m/2}} \exp\left(-\frac{\alpha}{m} \sum_{j=1}^m (h(x_j) - y_j)^2\right). \end{aligned}$$

As a result, the partition function $Z_\alpha(S, P)$ is,

$$\begin{aligned} Z_\alpha(S, P) &= (\pi m/\alpha)^{m/2} \int_h dh P(y|h, x) P_\theta(h) \\ &= (\pi m/\alpha)^{m/2} \mathcal{N}(y|m_\theta(x), k_\theta(x, x') + \frac{m}{2\alpha}I), \end{aligned}$$

We apply the GP base-learner Q on the the observed data S_i of task τ_i . For notation simplicity, let us denote $Q_i(h^i|S_i, P) = \mathcal{N}(\mu_i, K_i)$, where h^i denotes the model hypothesis (predictions) of the m_i examples in S_i . Then we have,

$$\begin{aligned} \hat{L}(Q_i, S_i) &= \frac{1}{m_i} \int Q_i(h^i)(y^i - h^i)^\top (y^i - h^i) dh^i \\ &= \frac{1}{m_i} (y^{i\top} y^i - 2\mu_i^\top y^i + \mu_i^\top \mu_i + \text{tr}(K_i)), \end{aligned}$$

where y^i denotes the labels of the m_i examples in S_i .

The hyper-prior $\mathcal{P}(P_\theta) := \mathcal{P}(\theta) = \mathcal{N}(\theta|0, \sigma_0^2 I)$ is an isotropic Gaussian defined over the network parameters θ , where we take $\sigma_0^2 = 3$ in our numerical experiments. The MAP approximated hyper-posterior takes the form of a delta function, where $\mathcal{Q}_{\theta_0}(P_\theta) := \mathcal{Q}_{\theta_0}(\theta) = \delta(\theta = \theta_0)$. As a result, we have

$$\begin{aligned} D_{KL}(\mathcal{Q}_{\theta_0} \parallel \mathcal{P}) &= \int d\theta \delta(\theta = \theta_0) \left(\frac{\|\theta\|^2}{2\sigma_0^2} + \frac{k}{2} \log(2\pi\sigma_0^2) + \log \delta(\theta = \theta_0) \right) \\ &= \frac{\|\theta_0\|^2}{2\sigma_0^2} + \frac{k}{2} \log(2\pi\sigma_0^2) + c, \end{aligned}$$

which combined with $\tilde{\xi}$ becomes the regularizer on the parameters θ_0 .

D.2 Experiment Details

In the Sinusoid experiment, the number of available examples per observed task $m_i \in \{5, 10, 30, 50, 100\}$. Under the setting of PACOH (Theorem 3), for each different m_i , we did a grid search on $\beta/m_i \in \{10, 30, 100\}$. Under the setting of PACMAML (Theorem 4), for each different m_i , we did a grid search on $\beta/m_i \in \{10, 30, 100\}$ and $\alpha/\beta \in \{0.1, 0.2, 0.3, 0.4, 0.5, 0.6\}$. We use a subset $S'_i \subset S_i$ with $m'_i = m$ to train the base-learner in PACMAML. For each hyperparameter setting β (and α), we trained 40 models. Each model is trained on 1 of the 8 pre-sampled meta-training sets (each containing $n = 20$ observed tasks) and each set is run with 5 random seeds of network initialization. The ultimate result for each β (and α) is the averaged result across all models of that setting. The hyperparameters $\tilde{\xi}$ and σ_0^2 in the hyper-prior ($\mathcal{P}(\theta) = \mathcal{N}(\theta|0, \sigma_0^2 I)$) are chosen to be $\tilde{\xi} = 1/(n\beta)$ and $\sigma_0^2 = 3$. To find the optimal model parameter θ_0 , we used the ADAM optimizer with learning rate 3×10^{-3} . The number of tasks per batch is fixed to 5 across all experiments. We run 8000 iterations for each experiment.

The experiments ran in parallel on several 56-core Intel CLX processors and each experiment runs on a single core. Each iteration in the PACOH and PACMAML setting takes about 0.03-0.06s and 0.07-0.14s to run, respectively, with the exact run-time varying for different number of tasks n and number of examples m_i .

D.3 Additional Results

We performed the 4-fold cross validation over the 20 target tasks to determine the optimal β for PACOH (Theorem 3) or the optimal α and β for PACMAML (Theorem 4). For the selected α and β from validation, we report the lowest test error the corresponding models can achieve. The results are plotted in Figure 3. For each setting, both the validation and test errors show the same trend, where the error with PACOH setting saturates earlier than that with PACMAML setting.

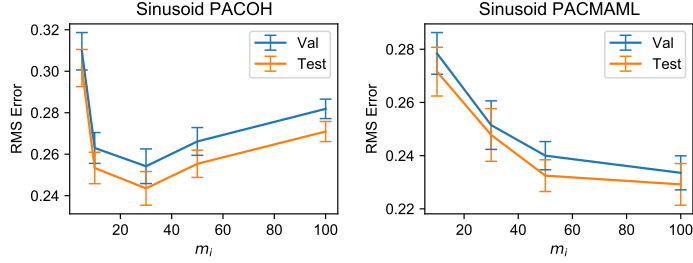


Figure 3: The validation and test error (error bars corresponding to standard errors) on the Sinusoid dataset under the settings of PACOH and PACMAML.

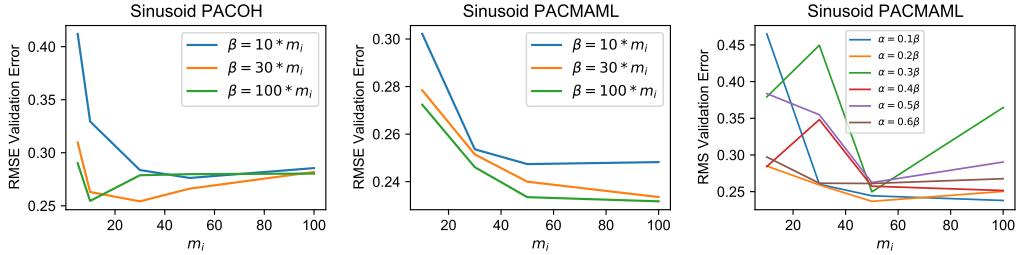


Figure 4: Left: β -dependence of the RMSE validation error under the PACOH (Theorem 3) setting. Middle and Right: β - and α -dependence of the RMSE validation error under the PACMAML (Theorem 4) setting. α is chosen as the optimal α in the middle plot. $\beta = 30 * m_i$ in the right plot.

m_i	5	10	30	50	100
β/m_i	100	100	30	30	100

Table 3: Optimal β under the setting of PACOH, based on the results of a 4-fold cross validation.

m_i	10	30	50	100
α/β	0.2	0.2	0.2	0.1
β/m_i	100	100	100	100

Table 4: Optimal α and β values under the setting of PACMAML, based on the results of a 4-fold cross validation.

In Table 3 and Table 4, we provide the optimal β (and α) for PACOH and PACMAML, respectively. In Fig. 4, we plotted the validation error for three different values of β we used. We see that for both PACOH and PACMAML, the error is large for a small $\beta/m_i = 10$. The error with $\beta/m_i = 30$ and $\beta/m_i = 100$ are similar for PACOH. For PACMAML, the error with $\beta/m_i = 100$ is slightly and consistently better than the error with $\beta/m_i = 30$. From the right figure of Fig. 4 we see that for PACMAML, given $\beta/m_i = 30$, α/β around 0.2 achieves lowest validation error.

D.4 Generalization Bound of PACMAML

When β/m_i is held as a constant, the Ψ_1 and Ψ_2 terms of $C(\delta, \lambda, \beta, n, m_i)$ in Eq.(17) becomes the same across all m_i and both PACOH (Eq. (10)) and PACMAML (Eq. (11)). Thus, we exclude

the Ψ_1 and Ψ_2 terms when comparing the bound values for different m_i and different setups PACOH and PACMAML. In Fig. 5 and 6 we show the value of each term and the total bound for PACOH and PACMAML obtained from the same set of experiments for Fig. 2-4. For both PACOH and PACMAML, all three terms W , $\tilde{\xi}D_{KL}$ and $\tilde{\xi} \log(1/\delta)$ tend to decrease with larger m_i . For PACOH, with the extra term Δ_λ that panalizes larger m_i , the total bound either always increases with m_i or first increases then saturates. For PACMAML, without the Δ_λ term, the total bound $W_2 + \tilde{\xi}D_{KL} + \tilde{\xi} \log(1/\delta)$ monotonically decreases vs. m_i .

In Fig. 7, we show the comparison between the total bound of PACOH and PACMAML. We see that for all $m_i > 5$, PACMAML has lower bound for all choices of β .

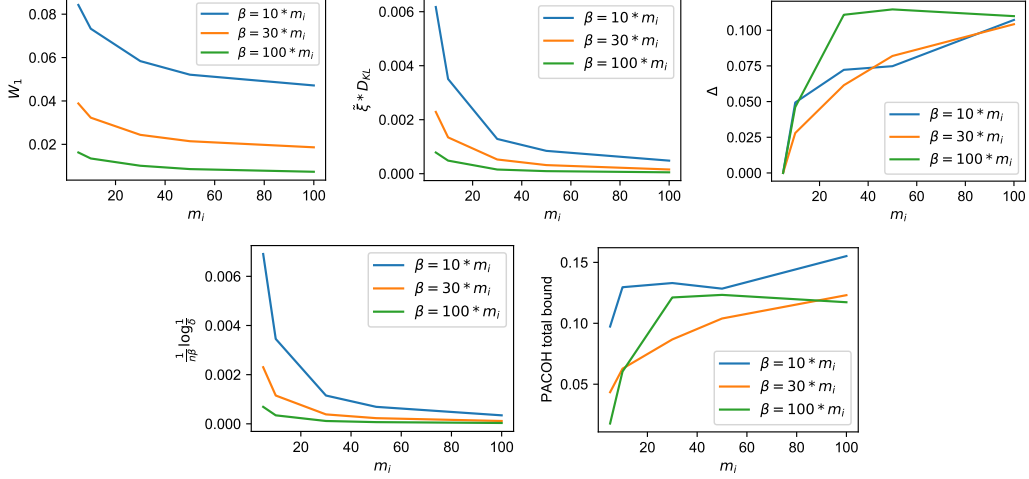


Figure 5: Values of W_1 , $\tilde{\xi}D_{KL}$ and Δ terms in the PACOH bound and the total value of the bound for $\beta/m_i \in \{10, 30, 100\}$.

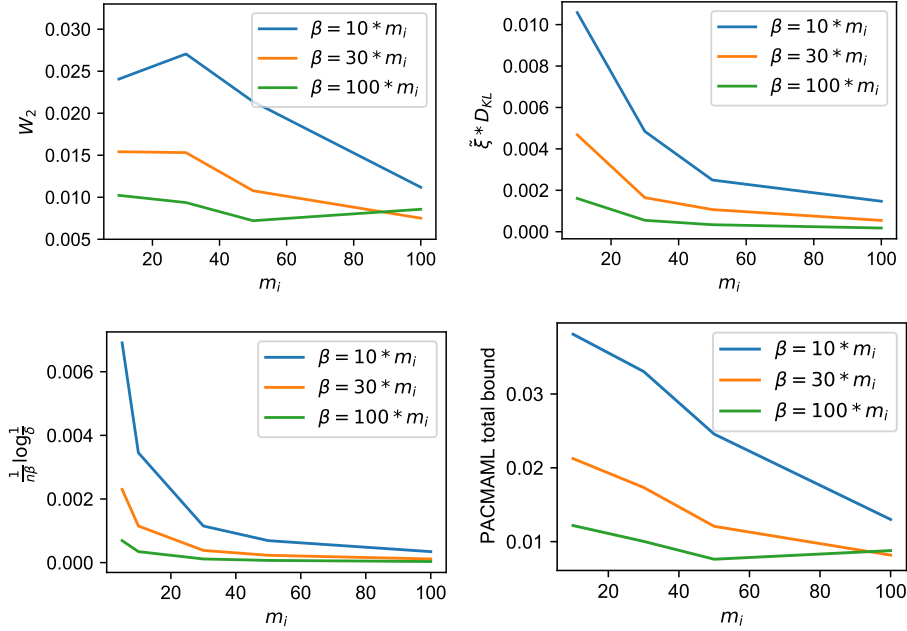


Figure 6: Values of W_2 and $\tilde{\xi}D_{KL}$ terms in the PACMAML bound and the total value of the bound for $\beta/m_i \in \{10, 30, 100\}$. α for each m_i is set to the optimal value according to Fig. 4.

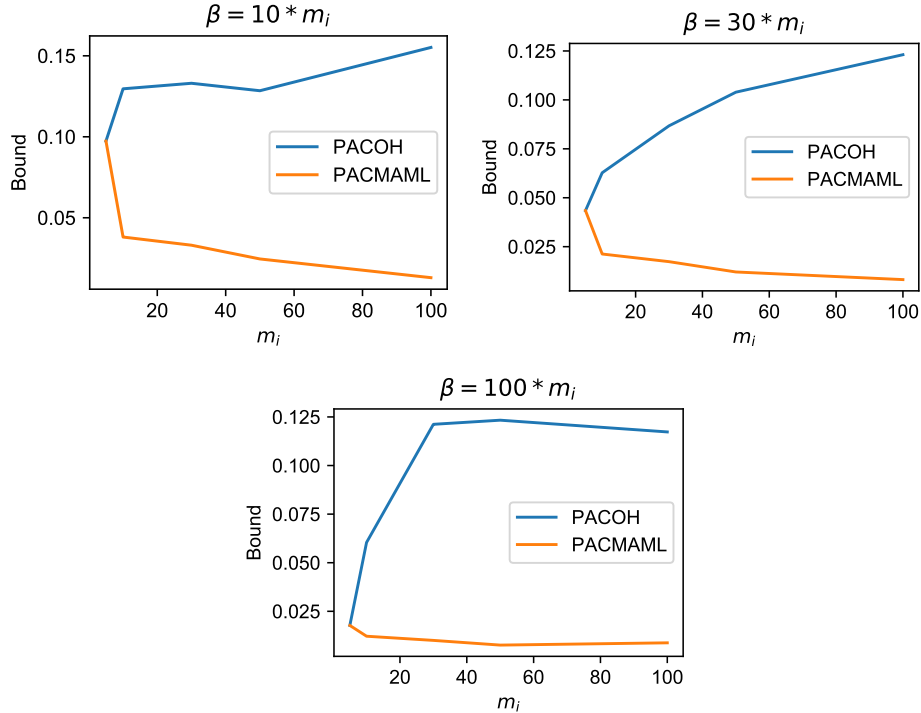


Figure 7: Comparison of the values of PACOH and PACMAML bound for $\beta/m_i \in \{10, 30, 100\}$. α for each m_i for PACMAML is set to the optimal value according to Fig. 4.

D.5 Experiment for Reptile and MAML

We also experimented with meta-learning algorithms that use Dirac-measure base-learners, by implementing the Reptile (with optimal \mathbf{q}^*) and the MAML algorithms following the equations of Section 3.2.

Reptile follows the same experiment setting as PACOH. MAML follows the same experiment setting as PACMAML where $S'_i \subset S_i$, $m'_i = m$. In order to compute the optimal \mathbf{q}_i^* for Reptile, we use an L-BFGS optimizer in the inner loop with `lr = 5e-3`, `history_size = 10`, `max_iter = 10`. Other experiment setting and hyperparameter selection procedure are the same as those in Section D.3.

The results of the 4-fold cross validation are plotted in Fig. 8. The errors of Reptile and MAML follow a very similar trend to the ones with non-Dirac measure base-learners under PACOH and PACMAML setting, respectively (Fig. 3). However, the models with non-Dirac measure base-learners appear to have lower generalization errors than the ones with Dirac measure base-learners (i.e. Reptile and MAML).

E Experiment Details of Image Classification

For most hyperparameters, we followed the same default values as in [Finn et al., 2017]. In Table 5, we listed the hyperparameters that we did grid search, and their chosen value based on the meta-validation performance. For the inner learning rate, the search space was $\{0.1, 0.03, 0.001, 0.003\}$ for FOMAML, MAML, and PACMAML; the search space was $\{0.1, 0.03, 0.001, 0.003, 0.001, 0.0003, 0.0001\}$ for BMAML and PACOH. For the meta-learning rate, we used the default 0.001 for FOMAML, MAML and PACMAML; and searched over $\{0.001, 0.0003, 0.0001, 0.00003\}$ for BMAML and PACOH. For α , we searched over $\{10, 1.0, 0.1\}$ for BMAML, PACOH, PACMAML. We also tried two gradient descent methods in the inner loop: Vanilla GD and ADAGRAD. We found that FOMAML and MAML worked better with Vanilla GD; while BMAML, PACOH and PACMAML worked better with ADAGRAD. σ^2 was fixed to 1 for

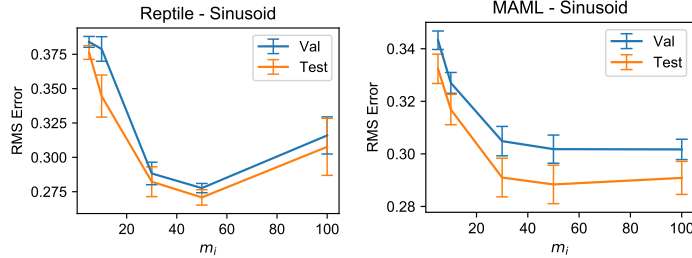


Figure 8: Mean and standard error of the validation and the test result for Reptile and MAML on Sinusoid. The results are obtained from cross-validation. The error bars in the figures represent the standard errors.

PACOH and PACMAML. The number of task per batch was 4 and the network filter size was 64. The total number of meta-training iterations was 60000 for all algorithms. We ran these tasks with 1 NVIDIA P100 GPU per job and each job takes about 2-3 hours to finish.

m_i	Hyper-parameter	FOMAML	MAML	BMAML	PACOH	PACMAML
10	outer learning rate	0.001	0.001	0.0001	0.0001	0.001
	inner learning rate	0.1	0.1	0.003	0.01	0.03
	α	-	-	1.0	10	1.0
20	outer learning rate	0.001	0.001	0.0001	0.0001	0.001
	inner learning rate	0.03	0.1	0.003	0.003	0.01
	α	-	-	0.1	1.0	1.0
40	outer learning rate	0.001	0.001	0.0001	0.0001	0.001
	inner learning rate	0.03	0.03	0.003	0.003	0.01
	α	-	-	0.1	1.0	10
80	outer learning rate	0.001	0.001	0.0001	0.0001	0.001
	inner learning rate	0.03	0.03	0.0003	0.003	0.01
	α	-	-	0.1	1.0	1.0

Table 5: The final hyper-parameters of the algorithms in the Mini-imagenet task.

F Experiment Details of Natural Language Inference

We fixed $\sigma^2 = 0.0004$, which equals to the variance of the BERT parameter initialization. The hyper-parameter α is decided by a grid search over $\{10^2, 10^3, 10^4, 10^5, 10^6, 10^7\}$ based on the performance on the meta-validation dataset. The inner loop learning rate is 0.001 for all algorithms. We used 50-step Adagrad optimizer in the inner-loop because it has automatic adaptive learning rate for individual variables which is beneficial for training large models. For the outer-loop optimization, we used the ADAM optimizer with learning rate 10^{-5} . The final hyperparameters are reported in Table 6. In the few-shot learning phase, we ran the ADAM optimizer for 200 steps with learning rate 10^{-5} on the adaptable layers. We ran the tasks with 16 TPUs(v2) per job.

Hyper-parameter	MAML	BMAML	PACOH	PACMAML
inner learning rate	0.001	0.001	0.001	0.001
v	12	12	12	11
m'_i	32	64	256	64
m_i	256	256	256	256
α	-	10^3	10^4	10^4
tasks per batch	1	1	1	1
meta-training iteration	10000	10000	10000	10000

Table 6: The final hyper-parameters in the NLI tasks.

In Table 7 we report the detailed classification accuracy on the 12 NLI tasks with their standard errors.

Task name	N	k	MAML	BMAML	PACOH	PACMAML
CoNLL	4	4	63.0±1.4	61±2.3	62.1±2.2	68.8±1.6
		8	74.1±1.8	68±1.9	74.9±1.2	79.5±1.1
		16	81.6±0.6	77.9±1.4	83±0.7	84.5±0.6
MITR	8	4	51.3±1.8	47.5±1.9	55.9±1.6	60.6±1
		8	69.1±2.1	64.2±1.3	71.8±0.8	70.9±1
		16	78.7±1.1	72.2±1.3	78.1±0.6	80±0.6
Airline	3	4	60.1±2.0	53±2.7	60.1±3.1	60.5±1.9
		8	64.7±2.7	67.4±2.2	65±1.5	65.4±1.7
		16	68.4±2.2	66.7±2.6	69.6±1.3	69.9±1.1
Disaster	2	4	56.3±0.5	58.7±3.1	58.7±2.6	63.3±1.3
		8	61.5±0.7	64.1±2.3	64.1±2.4	63.9±2.9
		16	67.7±0.4	69.4±2.0	71.3±1.7	71.1±1.6
Emotion	13	4	13.7±2.1	13.9±0.5	13.8±0.5	13.7±0.7
		8	15.8±1.9	14.6±1.1	15±0.6	15.8±0.6
		16	16.7±0.9	15.6±0.7	17.2±0.7	16.8±0.5
Political Bias	2	4	58±2.1	58±2.0	58.8±2.6	59.9±2.1
		8	60.7±1.9	61±1.9	62.1±1.5	62±1.9
		16	64.6±0.9	63.5±1.2	63.8±1.2	66±1
Political Audience	2	4	52.2±0.9	54.9±0.7	53.1±0.9	53.4±1.3
		8	56.1±1.5	55.9±1.1	56±1.3	56±1.2
		16	56.5±1.2	56.9±1.3	60±0.9	59.6±1
Political Message	9	4	18.9±0.8	17.4±0.6	19.2±0.7	19.3±0.6
		8	22.3±0.7	19.3±0.8	22.3±0.6	22.6±0.5
		16	24.3±0.8	21.6±0.4	24.9±0.4	25.5±0.8
Rating Books	3	4	58.7±2.1	56.2±2.8	59±2.3	56.8±3
		8	61.3±2.7	55.1±2.7	64.2±2	61.6±1.5
		16	62±1.3	66.6±2.1	63±2.1	60.4±2.7
Rating DVD	3	4	49.5±3.0	53.7±2.7	53.7±2.1	52.4±1.5
		8	53.2±1.6	51.8±2.4	54.7±2	56±2
		16	54.7±1.2	57.2±1.5	55.4±1.3	60±1.4
Rating Electronics	3	4	46.9±3.1	44.6±1.9	53.3±1.7	52.4±2
		8	52.5±1.6	54.1±1.6	55.6±2	56.1±1.3
		16	54.7±1.8	56.6±1.8	57.5±1.5	58.2±0.7
Rating kitchen	3	4	49.9±2.4	48.3±2.1	57.9±1.3	57.8±2
		8	50.9±2.8	49.5±3.1	52.3±2.2	58.3±1.5
		16	58.7±1.5	54.2±1.8	54.8±1.8	58.1±2.5
Overall average	-	4	48.21	47.27	50.47	51.58
		8	53.52	52.08	54.83	55.68
		16	57.38	56.53	58.22	59.18

Table 7: Classification accuracy and standard error on the 12 NLI tasks.